Role of Stress Fiber–like Structures in Assembling Nascent Myofibrils in Myosheets Recovering from Exposure to Ethyl Methanesulfonate

Parker B. Antin,*‡ Sohei Tokunaka,* Vivianne T. Nachmias,* and Howard Holtzer*

*Department of Anatomy, University of Pennsylvania School of Medicine, Philadelphia, Pennsylvania 19104; ‡Department of Cell Biology and Anatomy, Cornell University Medical College, New York, New York, 10021. Dr. Tokunaka's present address is Department of Urology, Asahikawa Medical College, Asahikawa 078-11, Japan.

Abstract. When day 1 cultures of chick myogenic cells were exposed to the mutagenic alkylating agent ethyl methanesulfonate (EMS) for 3 d, 80% of the replicating cells were killed, but postmitotic myoblasts survived. The myoblasts fused to form unusual multinucleated "myosheets": extraordinarily wide, flattened structures that were devoid of myofibrils but displayed extensive, submembranous stress fiber–like structures (SFLS). Immunoblots of the myosheets indicated that the carcinogen blocked the synthesis and accumulation of the myofibrillar myosin isoforms but not that of the cytoplasmic myosin isoform.

When removed from EMS, widely spaced nascent myofibrils gradually emerged in the myosheets after 3 d. Striking co-localization of fluorescent reagents that stained SFLS and those that specifically stained myofibrils was observed for the next 2 d. By both immunofluorescence and electron microscopy, individual nascent myofibrils appeared to be part of, or juxtaposed to, preexisting individual SFLS. By day 6, all SFLS had disappeared, and the definitive myofibrils were displaced from their submembranous site into the interior of the myosheet. Immunoblots from recovering myosheets demonstrated a temporal correlation between the appearance of the myofibrillar myosin isoforms and the assembly of thick filaments. The assembly of definitive myofibrils did not appear to involve desmin intermediate filaments, but a striking aggregation of sarcoplasmic reticulum elements was seen at the level of each I-Z-band. Our findings suggest that SFLS in the EMS myosheets function as early, transitory assembly sites for nascent myofibrils.

DEFINITIVE muscle cells selectively synthesize a complex set of contractile proteins that interact precisely to form the relatively invariant striated myofibril. Major myofibrillar components include muscle-specific isoforms such as myosin heavy and light chains, alpha-actin, tropomyosins, troponins, alpha-actinin, titin, nebulin, and M-band proteins (see articles cited in reference 52). These myofibrillar isoforms are synthesized and assembled into definitive sarcomeres arranged in tandem during the earliest stages of myofibrillogenesis in vivo and in vitro (2, 21, 33). With maturation there is an enormous increase in the numbers of interdigitating thick and thin filaments in each nascent myofibril, the total number of individual myofibrils, and the number of new sarcomeres, which apparently are added at the ends of the elongating myofibrils (1, 14, 31, 33, 36, 68).

An intriguing aspect of myofibrillogenesis is that many of the muscle-specific isoforms correspond to a related set of proteins that are synthesized in virtually all cells, including presumptive myoblasts, chondroblasts, nerve cells, fibroblasts, and endothelial cells. In nonmuscle cells these constitutive contractile protein isoforms are not present in a stable arrangement but may interact to form stress fibers and/or microfilaments, depending upon the degree of cell spreading, motility, attachment to the substrate, and hemodynamic factors (23, 33, 37, 42, 43, 54, 69–72). When present, stress fibers and their associated dense bodies display periodicities suggestive of sarcomeres (20, 27, 36, 39, 59). Similarly, desmin, the muscle intermediate filament isoform, is closely related in structure and amino acid sequence to vimentin, the intermediate filament protein synthesized by many mesenchymally derived cells, as well as by presumptive neurons and cultured epithelial cells (5, 19, 24, 25, 32, 62, 63).

Postmitotic mononucleated myoblasts and myotubes synthesize both the constitutive and muscle-specific contractile protein isoforms and also both desmin and vimentin (5, 8, 16, 18, 19, 44, 46, 56, 57). Although several workers have failed to document an obvious role for desmin in the early assembly of striated myofibrils in skeletal muscle (5, 32–36, 64–66), there is evidence that the earliest stages of myofibrillogenesis involve the nonmuscle contractile isoforms that constitute stress fibers and microfilaments. In skeletal myogenic cells the close association between the plasma membrane and the first forming myofibrils has long been noted (21, 22, 29, 31, 36, 38). It has been emphasized that a given

myofibril that binds antibodies to myofibrillar myosin in A-bands and tropomyosin in I-bands always terminates at both ends as a nonstriated structure in the cell's growth tips (31, 33, 36, 53). Such nonstriated ends of myofibrils have been observed in the growth tips of postmitotic mononucleated myoblasts and in myotubes, where they associate closely with structures that bind antibodies to nonmuscle myosin (14, 18). It has also been reported that in spreading cardiac myocytes antibodies to alpha-actinin bind to Z-bands of definitive sarcomeres and also to the nonstriated "ends" of such sarcomeres with a punctate periodicity characteristic of stress fibers (58).

A recent study of myofibrillogenesis in cardiac myocytes (14) has confirmed the observations made on skeletal muscle cells and in addition has contributed the following: (*a*) stress fiber–like structures (SFLS[1]; see also reference 41) predated the emergence of nascent myofibrils; (*b*) each of the first detectable nascent myofibrils was invariably associated with a single preexisting SFLS; and (*c*) as individual nascent myofibrils matured, the SFLS disappeared. These results showed that SFLS were transient structures and that mature cardiac myocytes normally do not have SFLS, and suggested that in cardiac myocytes a single SFLS functioned as a "nucleation site" for each definitive myofibril. As in skeletal muscle cells, early myofibril formation and the assembly of Z-bands in cardiac cells appeared to be independent of the distribution of desmin (5, 32, 35).

Possible interactions among stress fibers, microtubules, intermediate filaments, and myofibrils in cultured skeletal muscle are difficult to examine microscopically in normally developing myotubes since the cells are relatively thick and the assembly of myofibrils is relatively rapid. To circumvent these problems, we focused in this study on the topographical and temporal relationships of SFLS and nascent myofibrils in skeletal myogenic cells recovering from treatment with the mutagenic alkylating agent ethyl methanesulfonate (EMS). EMS alters myogenesis in a striking but reversible way (1, 34). While in EMS postmitotic myoblasts fuse into immense, inordinately flattened, multinucleated "myosheets." As judged by pulse labeling with [^{35}S]methionine, or by in vitro translation of total cellular RNA, these myosheets do not synthesize many of the muscle-specific contractile proteins. However, myosheets maintained in EMS continue to synthesize other cellular proteins at or above control levels. After EMS is removed, recovering myosheets remain flattened while they slowly, over a period of days, initiate the synthesis of the muscle-specific contractile proteins and assemble them into long, narrow, definitively striated myofibrils. These myofibrils contract spontaneously and are well separated from one another and easily observed due to the extreme thinness (<1 μm) of the myosheets. The favorable optical properties and the relatively protracted period required for myofibrillar assembly after removal of the carcinogen render myosheets ideal for studying the relationship of early forming myofibrils to other cytoskeletal components.

We find that whereas EMS selectively blocks the emergence of myofibrillar structures, it does not block the emergence of a rich sarcoplasmic reticulum (SR) and T-system or of longitudinally disposed desmin intermediate filaments. During recovery from EMS the earliest nascent myofibrils assemble in close association with transitory, submembranous SFLS. As thick and thin filaments are added to the periphery of the nascent myofibrils, they are displaced to the cell's interior, and SFLS disappear. Our impression therefore, is that SFLS are, or function as, an initial but transitory site for the organization and assembly of definitive myofibrils.

[1] *Abbreviations used in this paper:* CBM, chick brain myosin; EMS, ethyl methanesulfonate; FITC, fluorescein isothiocyanate; MS LMM, muscle-specific light meromyosin; Rho-, rhodamine labeled; SFLS, stress fiber–like structure; SR, sarcoplasmic reticulum.

Materials and Methods

Cell Culture

Primary cultures of mononucleated cells were prepared from breast muscles of 11-d chick embryos as described (7, 11) with slight modifications. Small fragments of breast muscle were incubated for 20 min in calcium-magnesium-free Hank's balanced salt solution containing 1.0% trypsin (Gibco, Grand Island, NY). After removal of the trypsin solution, cells were dispersed by repeated pipetting in culture medium (10% horse serum, 10% embryo extract, 50 U/ml penicillin, 50 μg/ml streptomycin, and 250 μg/ml fungizone in Eagle's minimum essential medium with Earles salts; Gibco). The resulting suspension was passed through a double thickness of lens paper in a Swinney adapter. Cells were plated onto collagen or gelatin-coated Aclar (Allied Chemical Corp., Pottsville, PA) coverslips in 35-mm tissue culture dishes at 5×10^5 cells/ml. EMS (methanesulfonic acid, ethyl ester; Sigma Chemical Co., St. Louis, MO) was added to the medium of some cultures on day 1 (final concentration, 7.5 mM), and both control and EMS-treated cultures were fed daily using fresh medium with or without EMS. After 3 d of exposure to EMS, some cultures were immediately processed for immunofluorescence or electron microscopic analysis; parallel cultures were allowed to recover in normal medium for 1–10 d before processing.

Antibodies

The properties of the antibodies against muscle-specific light meromyosin (anti-MS LMM) and desmin (anti-desmin) have been described. In brief, in immunoblots prepared using total extracts of skeletal or cardiac muscle, anti-MS LMM binds only to the 200-kD myosin band (see Fig. 13*b*). In similar immunoblots prepared from smooth muscle or fibroblasts, the anti-MS LMM does not bind to the 200-kD myosin band. In cytoimmunofluorescence, anti-MS LMM binding is restricted to the myofibrillar A-bands in postmitotic myoblasts, myotubes, and cardiac myocytes (5, 8, 12, 15). Anti-MS LMM does not stain the myosin in presumptive myoblasts, smooth muscle, fibroblasts, or other cell types examined. A monoclonal antibody prepared against chicken skeletal myosin (anti-MHC) was the gift of Dr. Frank Pepe (University of Pennsylvania). Anti-MHC binds exclusively to the A-bands of skeletal and cardiac myofibrils and does not bind to myosin in smooth muscle, presumptive myoblasts, or other cell types examined. The antidesmin binds to intermediate filaments in skeletal, cardiac, and smooth muscle (6) but not to the vimentin intermediate filaments in fibroblasts (4, 5, 19). Antibody against smooth muscle alpha-actinin was a generous gift from Dr. S. Craig (Johns Hopkins University) and has been described previously (10). In skeletal myogenic cultures, this anti-alpha-actinin has been shown to bind to the Z-bands of postmitotic mononucleated myoblasts and myotubes (2). Antibody was produced against chick brain myosin (anti-chick brain myosin [CBM]) by using column purified myosin from chick brain (40) for primary injection of rabbits. Pure myosin heavy chain, obtained by eluting the appropriate band from a 7% SDS gel, was used for boosting the primary injection four times. IgG was purified and found to react with the heavy chain of myosin from fibroblasts and EMS-treated skeletal myosheets but not with myosin heavy chains from chick myofibrils as demonstrated by immunoblot (Fig. 13*d*). Immunofluorescence localization of CBM was limited to stress fibers of chick fibroblasts and EMS myosheets; myofibrils did not bind the anti-CBM (34, 35). Antitubulin was purchased from Miles Laboratories Inc. (Naperville, IL).

Immunoblots

Whole cell homogenates of control, EMS-treated, and EMS-recovering cultures were mixed with 1 vol 2× Laemmli sample buffer containing 10 mM EDTA, 10 mM benzamidine, 10 μg/ml Trasylol, and 0.2 mM phenylmethylsulfonyl fluoride as protease inhibitors, and 10% 2-mercaptoethanol, boiled for 3 min, and clarified by centrifugation. Aliquots equalized to DNA content were separated by one-dimensional SDS PAGE in 1.2-mm thick gels, and the separated proteins were transferred electrophoretically to nitrocellulose filters in a Bio-Rad apparatus (Bio-Rad Laboratories, Richmond, CA). Filters were preincubated for 30 min in wash buffer (0.15 M sodium chloride, 0.5% Nonidet P = 40, 0.2% sodium azide, 5% bovine serum albumin in 0.05 M Tris HCl, pH 8.0), and incubated with appropriate serum at 1:200 or 1:500 dilution.

Bound rabbit antibodies were localized by incubation for 30 min with goat anti-rabbit IgGs at 80 μg/ml in wash buffer, then incubated for 30 min with rabbit peroxidase-anti-peroxidase complexes at a 1:200 dilution (Cappel Laboratories, Cochranville, PA) in wash buffer. Peroxidase activity was detected by the diaminobenzidine reaction as described (61). For optimal transfer of myosin heavy chains, low percentage gels (e.g., 7%) were used and transfer times were increased to 48 h.

Fluorescence and Electron Microscopy

Processing of cells for immunofluorescence staining was carried out as described (5, 62), with minor modifications. In brief, cultures were rinsed with phosphate-buffered saline (PBS; 5 mM sodium phosphate, 0.15 M NaCl [pH 7.3]) and fixed for 3 min in 2.5% formaldehyde in PBS. The cells were then rendered permeable and soluble proteins were extracted, using PBS containing 0.5% Triton X-100 (Sigma Chemical Co.). This solution was used for this step and all subsequent antibody "washes" and was replaced three times for a total of at least 30 min during each washing step. Various sequences of antibody or reagent incubations were used to produce the several double-stained preparations analyzed in this study. For antidesmin, anti-CBM, anti-MHC, and anti-alpha-actinin, the indirect immunofluorescent technique was used, whereas the fluorescein isothiocyanate (FITC)-labeled anti-MS LMM was visualized directly. To stain the same cells with anti-MS LMM and another rabbit antibody, a previously described procedure was used (5, 18, 62). The appropriate dilution of the antibody to be visualized indirectly was applied first. This and all other antibody incubations were carried out for 30–40 min at 37°C in a humid chamber. After the primary antibody incubation, cells were washed three times, incubated with secondary antibody (rhodamine-labeled goat anti-rabbit IgG, Cappel Laboratories), and washed again. Before anti-MS LMM was applied, the cells were incubated for 15–20 min at room temperature in a 1:5 dilution of normal rabbit serum in PBS to saturate exposed goat anti-rabbit IgG sites. Cells were then incubated with anti-MS LMM, washed, and mounted using 1:1 glycerol/PBS. Rhodamine-labeled phalloidin (Rho-phalloidin, Molecular Probes, Inc., Junction City, OR), which binds specifically to F-actin (71), was used to visualize microfilaments in the form of stress fibers and thin filaments within myofibrils. In antibody-stained preparations counterstained with Rho-phalloidin, fluorescein was used for the antibody visualization. After the final wash, cultures were rinsed repeatedly with PBS, incubated for 20 min at room temperature in 10 U/ml Rho-phalloidin in PBS, washed several times in PBS, and mounted as above. Antitubulin staining for microtubules was performed as previously described (2, 50). In some preparations, the DNA binding fluorochrome, bisbenzimide Hoechst 33258, was used to stain nuclei (62). Cells were examined with a Zeiss epifluorescence microscope using excitation filters for either fluorescein or rhodamine fluorescence and a specially designed short band pass barrier filter for fluorescein that we have determined eliminates bleedthrough between channels.

For electron microscopy, cells were prepared as previously described (13).

Results

Immunofluorescence Studies of Control and EMS-treated Myogenic Cultures

After 4-d in culture, control myotubes may be longer than 0.5 mm, occasionally branch, and have cross-sectional dimensions of 10–20 μm. Their numerous nuclei tend to line up in long rows and are equally distributed throughout the myotube. Large numbers of well-aligned, definitively striated myofibrils are present in all myotubes. We stress that in terms of numbers and sizes of individual myofibrils and nuclear-sarcoplasm ratio the myotubes that form in these primary cultures rival the morphological maturation observed in newly hatched chicks. Their degree of maturation greatly exceeds that of immortalized myogenic cell lines.

When 1-d cultures were treated with EMS (7.5 mM) for an additional 72 h, many replicating cells were killed. The number of surviving mononucleated cells after 3 d in the carcinogen—i.e., now 4-d cultures—was 5–15% of that in control cultures. Despite this cytotoxicity, EMS did not inhibit the fusion of postmitotic myoblasts into multinucleated structures. These structures were quite remarkable (Fig. 1; see also Figs. 4 and 5). They appeared as huge, thin sheets, often longer than 0.5 mm and wider than 0.2 mm, yet <1 μm thick; some had multiple extensions from the main sheet. A single structure might harbor >200 nuclei in a common sarcoplasm.

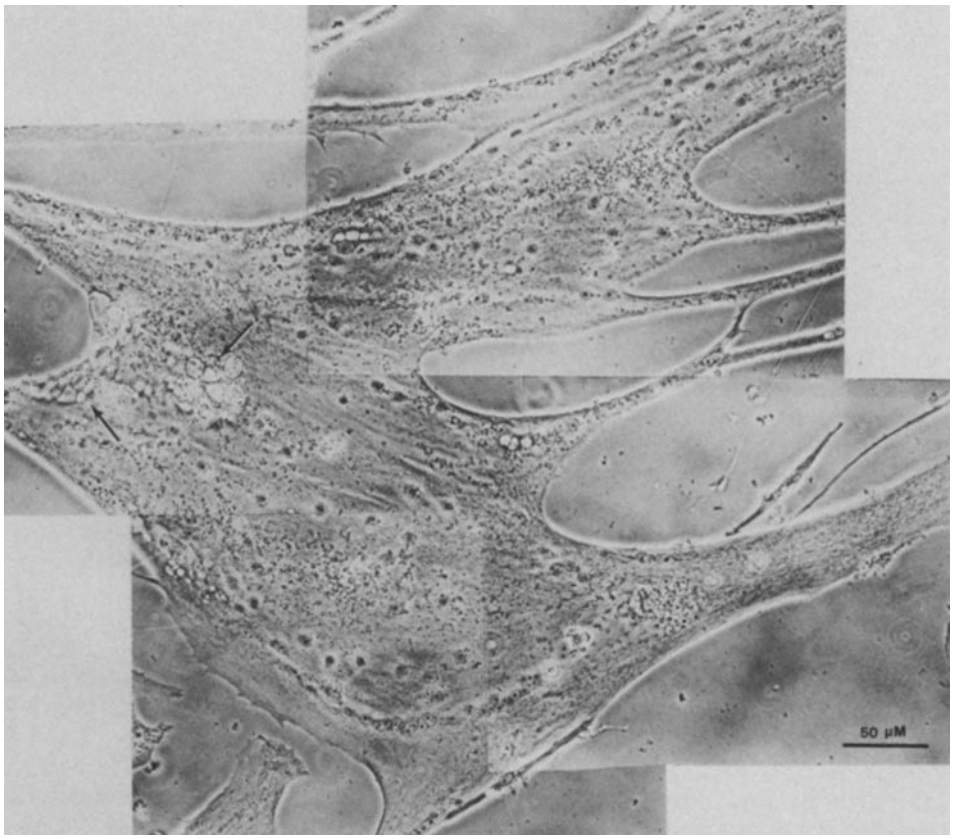

Figure 1. Composite, low-power phase micrograph of a single myosheet in a day 4 culture exposed to EMS for the previous 3 d. Larger and smaller myosheets are common. Note the virtual absence of mononucleated fibroblastic cells, though elsewhere in this culture dish modest numbers of such cells were present. Arrows point to aggregates of phase-lucent vacuoles.

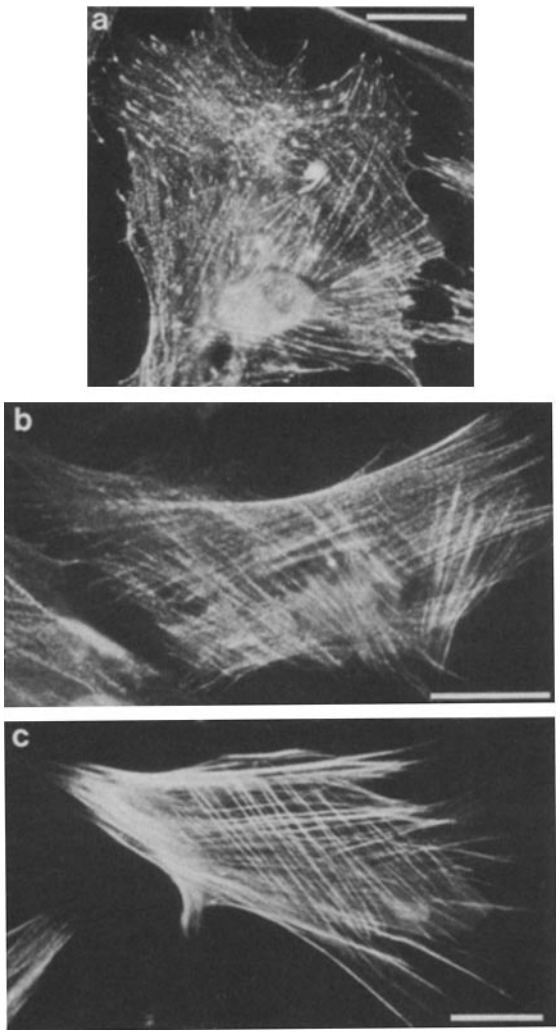

Figure 2. Spread, flattened mononucleated fibroblastic cells from day 4 control and day 4 EMS-treated cultures are indistinguishable when stained with fluorescent reagents. *a* is a fibroblastic cell from a control culture stained with anti-alpha actinin. *b* is a fibroblastic cell from an EMS-treated culture stained with anti-CBM. Note the interrupted staining pattern. This interrupted staining pattern, reflecting the presence of stress fibers, varies greatly with cell spreading. In less flattened cells the punctate pattern is not evident, and often in normal dense cultures the antibody stains the rounded fibroblastic cells diffusely. *c* is a fibroblastic cell from an EMS-treated culture stained with Rho-phalloidin. Bars, 20 μm.

The nuclei tended to aggregate in clusters of 20–60, often leaving sarcoplasmic domains >0.2-mm^2 devoid of nuclei. Spontaneous contractions were never observed in myosheets cultured in EMS.

There were no discernable differences between the stress fibers in the fibroblastic cells in the control cultures and the surviving spread fibroblastic cells in EMS cultures. The flattened adherent fibroblastic cells in both series displayed typical long stress fibers described by many investigators for a number of cell types. Antibodies to alpha-actinin (Fig. 2*a*) and to chick brain myosin (anti-CBM) (Fig. 2*b*) bound to these stress fibers in a punctate pattern. Measurements at higher magnifications showed a periodicity of 0.6–1.3 μM, although the fluorescent "bands" along stress fibers visualized by staining with anti-CBM were broader than those obtained by staining with anti-alpha-actinin. Rho-phalloidin stained stress fibers uniformly rather than in a punctate fashion (Fig. 2*c*). Stress fibers in the fibroblastic cells in control and EMS-treated cultures did not bind anti-MS LMM or anti-MHC (1, 8, 15).

Although stress fibers in fibroblastic cells appeared identical in treated and untreated cultures, there were striking differences in their presence or absence between control myotubes and EMS myosheets. Stress fibers were conspicuously absent over the length of the long, cylindrical body of day 4 myotubes stained with anti-CBM, Rho-phalloidin, or anti-alpha actinin (Fig. 3, *a*, *c* and *d*). Only in the growth tips and in those flattened regions that adhered to the substrate did the fluorescent reagents bind to structures in control myotubes with the properties of stress fibers.

In contrast, myosheets in day 4 cultures treated with EMS displayed numerous prominent well-separated fibrils that morphologically were indistinguishable from stress fibers (Fig. 4, *a*, and *c–f*). They tended to run parallel to the long axis and extended throughout the entire length and breadth of the EMS myosheet. The distances between individual fibrils and the degree of branching varied greatly. Anti-alpha actinin (Fig. 4, *a* and *f*) or anti-CBM (Fig. 4, *c* and *d*) staining revealed filaments with 0.6–1.3-μm periodicity. Filaments stained uniformly with Rho-phalloidin (Fig. 4, *e*) but did not stain with anti-MS LMM (Fig. 4*b*) or anti-MHC. In brief, 100% of the day 4 EMS myosheets, in contrast to day 4 myotubes, displayed structures that were indistinguishable from the stress fibers in fibroblasts after being stained with anti-CBM, anti-alpha-actinin, or Rho-phalloidin. These structures are SFLS (2, 15; see also reference 41).

There was a dramatic difference with respect to the presence or absence of striated myofibrils in day 4 control myotubes and day 4 EMS myosheets. Control myotubes contained innumerable striated myofibrils (Fig. 3, *b–d*), whereas myofibrils were not detectable in day 4 EMS myosheets (Figs. 4*b* and 5, *b* and *d*). A more detailed analysis of Figs. 3 and 4 illustrated the following salient points: (*a*) anti-CBM failed to stain myofibrils in control myotubes but stained SFLS in EMS myosheets in a punctate fashion (Figs. 3*a* and 4, *c* and *d*); (*b*) anti-alpha-actinin stained Z-bands of control myofibrils with a periodicity of 2.3–2.7 μm, whereas it stained SFLS in myosheets with a periodicity of 0.6–1.3 μm (Figs. 3*d* and 4, *a* and *f*); (*c*) Rho-phalloidin staining resulted in different but regular repeat patterns involving striations in both A- and I-bands of control myofibrils, whereas it continuously stained SFLS of EMS myosheets, as it does stress fibers in nonmuscle cells (Figs. 2*c*, 3*c*, and 4*e*).

The localization of antibodies to other fibrous structures was also examined. Antibodies to the desmin and vimentin intermediate filament proteins bound largely to longitudinally oriented filaments in both 4 day control myotubes (5) and in EMS myosheets (Fig. 5*c*). The dramatic shift in binding of antidesmin from longitudinal filaments to largely transverse striations associated with the I-Z-band of mature myofibrils was first observed in myotubes in day 6 and older control cultures (5, 24). Though largely longitudinally oriented, the intermediate filaments in myosheets often assumed a reticulated arrangement. No suggestion of transverse bands of intermediate filaments was observed in EMS myosheets. There was no obvious morphological evidence for interactions be-

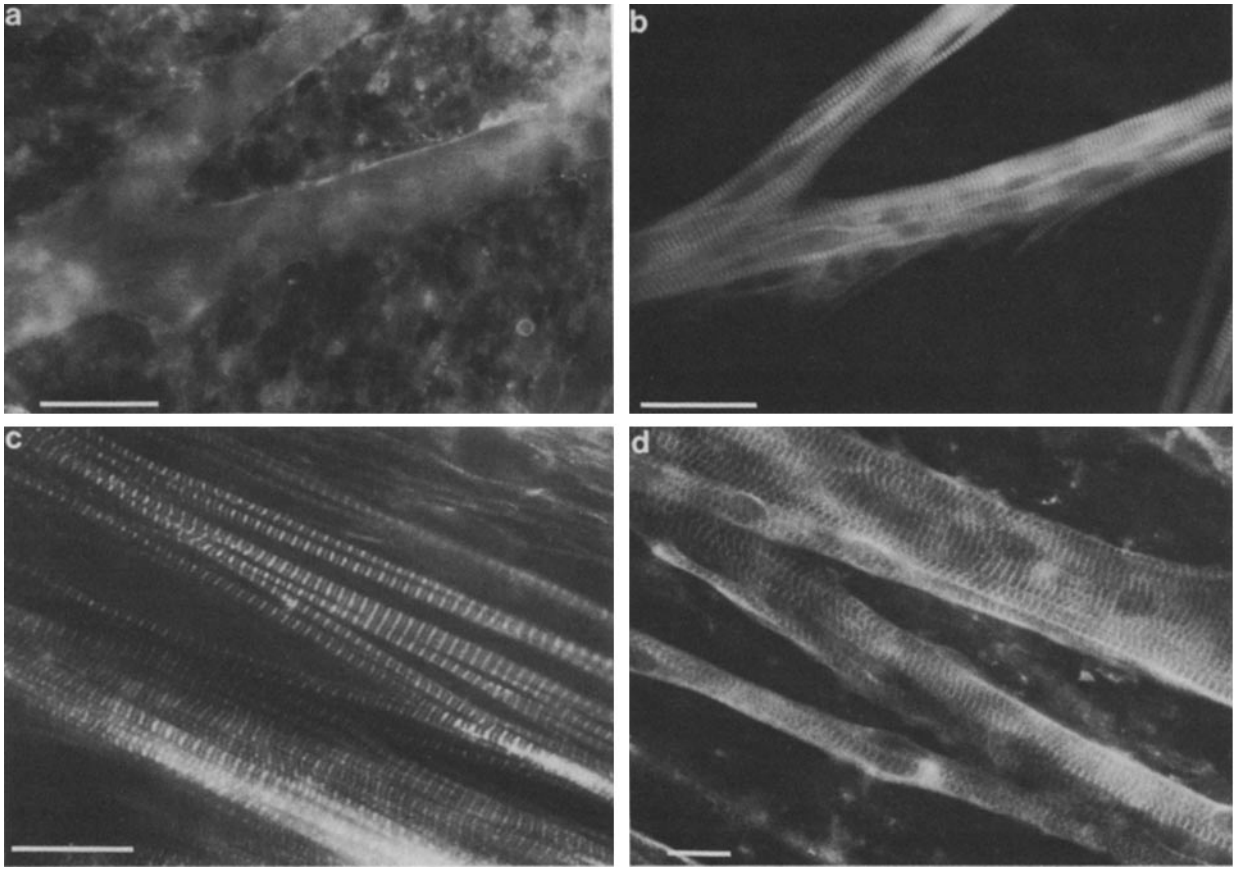

Figure 3. (*a–d*) Immunofluorescence micrographs illustrating the absence of stress fibers and the abundance of striated myofibrils in the body of myotubes from day 4 cultures. *a* and *b* are of the same microscopic field using the appropriate excitation and barrier filters to visualize rhodamine and fluorescein, respectively. The cells are stained with unlabeled anti-CBM (*a*) and FITC-labeled anti-MS LMM (*b*); the former is visualized by the indirect technique using rhodamine-labeled IgG. Note the absence of stress fibers in both *a* and *b* and the failure of the anti-CBM to stain the numerous striated myofibrils revealed by the anti-MS LMM. Similar micrographs were obtained using anti-MHC (data not shown). The numerous rounded fibroblastic cells surrounding the Y-shaped myotube diffusely bind the anti-CBM but are not stained with the anti-MS LMM. Bar, 50 μm. *c* is a micrograph of two adjacent myotubes stained with Rho-phalloidin. Stress fibers as revealed by Rho-phalloidin staining of fibroblasts are not present in the body of myotubes. Note especially the curious fluorescent pattern of the individual myofibrils. This unexpected striated pattern is also found with mature glycinerated myofibrils (data not shown) and is dependent upon the extent of myofibril contraction. Bar, 20 μm. *d* is a micrograph of a myotube stained with anti-alpha-actinin illustrating the sharp staining of Z-bands. Again, note the absence of structures that could be identified as stress fibers in the body of these myotubes. Bar, 20 μm.

tween intermediate filaments and SFLS in either control myotubes or EMS myosheets.

Normal day 4 myotubes stained with antitubulin were difficult to interpret due to overlapping of the many longitudinally oriented microtubules. Fig. 5*a* illustrates the distribution of microtubules in two adjacent EMS myosheets. At higher magnification, it was not uncommon to follow a single microtubule for more than 50 μm in these myosheets. Myosheets did not exhibit obvious microtubule organizing centers, and obvious morphological associations of microtubules with SFLS, intermediate filaments or other cell organelles were not observed.

Electron Microscopic Studies of EMS-treated Myogenic Cultures

Stress fibers in the fibroblastic cells of both control and EMS-treated cultures appeared as bundles of microfilaments with interspersed, irregular dense bodies when viewed under the electron microscope. They subtended the plasma membrane at the lower, and to a much lesser extent the upper, surface. Comparable bundles were observed in control flattened 2–3-d myotubes. They disappeared within the next 24 h in normal myotubes and were absent throughout the cylindrical belly of day 4 and older myotubes. SFLS were confined to the growth tips and occasional lateral pseudopodial extensions in older normal myotubes.

In contrast, SFLS were exceedingly prominent in day 4 EMS myosheets (Fig. 6). Curiously, SFLS were almost exclusively associated with the upper or free surface of the myosheet rather than the surface facing the substrate. Well separated from one another in the belly of the myosheet, the conspicuous long SFLS tended to converge in the myosheets' growth tips. Although various fixation and counterstaining procedures were used (45). SFLS were not observed coursing through the cytoplasm from the upper to the lower surface of the EMS myosheets. These electron microscopic studies confirmed the cytoimmunofluorescence observation: SFLS, absent from the body of normal maturing cylindrical day 4 and older myotubes, were conspicuous throughout the flattened day 4 EMS myosheets.

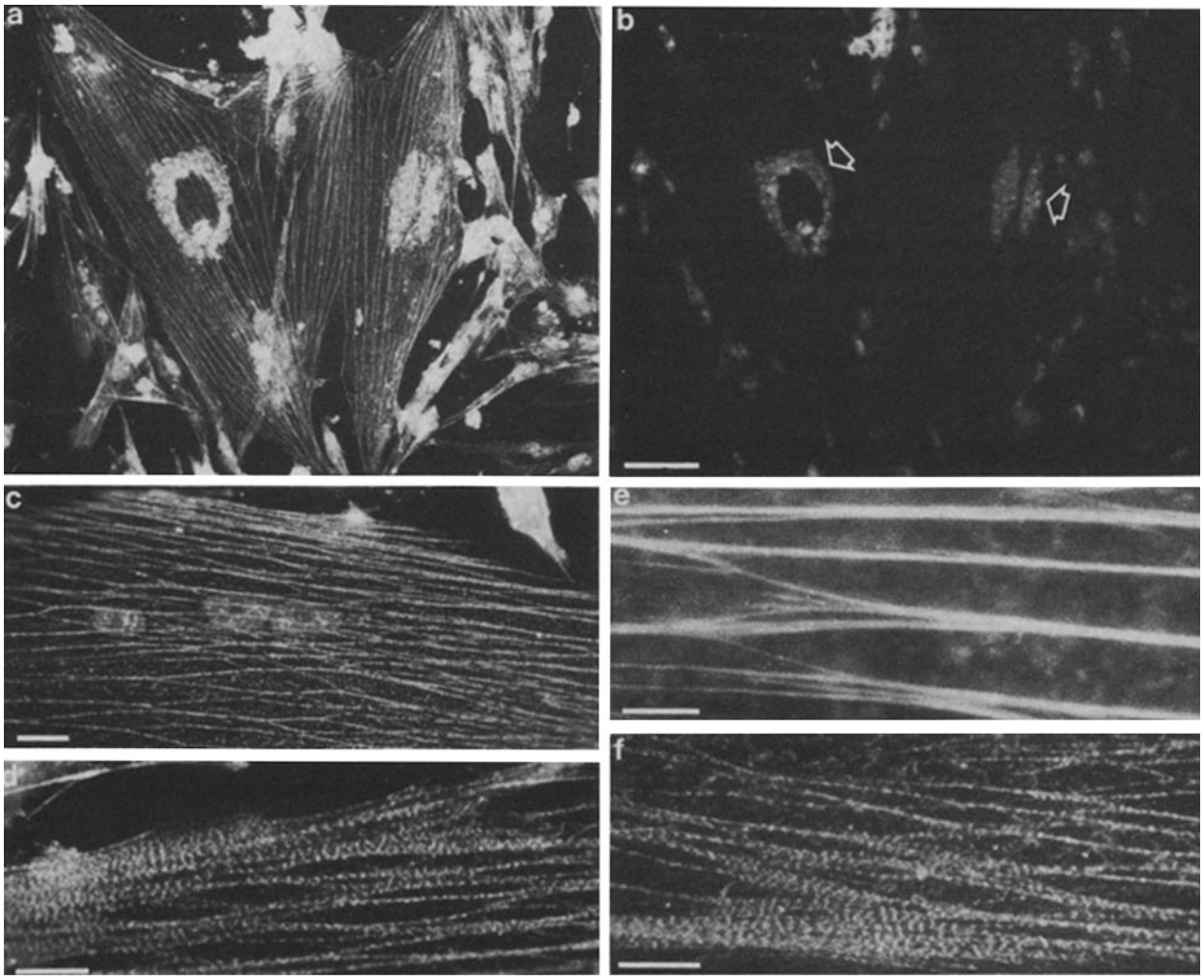

Figure 4. Immunofluorescence micrographs illustrating the presence of prominent stress fibers throughout the body of, and the total absence of any myofibrillar structures from, EMS myosheets. *a* and *b*, visualizing the same microscopic field, are of two adjacent, possibly fused, EMS myosheets stained with anti-alpha-actinin (*a*) and with anti-MS LMM plus bisbenzamid H to stain nuclei (*b*). *a* and *b* are viewed using the appropriate filters to visualize rhodamine and fluorescein, respectively. Note the conspicuous, long SFLS revealed by the anti-alpha-actinin staining (*a*). Even at this low magnification comparable structures can be detected in the surrounding flattened fibroblastic cells. The total absence of antigen to bind the anti-MS LMM (*b*) is obvious. Arrows point to clusters of nuclei (the anti-alpha-actinin used in this study routinely bound to nuclei as seen in *a*). (*a* and *b*) Bar, 50 μm. *c* visualizes the edge of an EMS myosheet stained with anti-CBM. The punctate staining pattern of the bifurcating SFLS is evident. Bar, 10 μm. (*d–f*) High magnification micrographs of EMS myosheets stained with anti-CBM (*d*), Rho-phalloidin (*e*), and anti-alpha-actinin (*f*). Observe that the distance between individual SFLS can vary greatly. Bars, 10 μm.

Without exception, day 4 control myotubes displayed numerous definitively striated myofibrils, consisting of tandem sarcomeres ~2.5 μm long. Most conspicuous in these control myotubes was the clear association of the well-developed SR with the I-Z region at all stages of myofibrillogenesis. The clusters of poorly aligned thick and thin filaments that characterize the early stages of myofibrillogenesis in day 2–3 control myotubes (21, 36, 37, 60) largely disappeared in day 4 myotubes, at which time the thick and thin filaments were organized into typical myofibrils with relatively sharp edges.

Consistent with the information in Figs. 4*b* and 5, *b* and *d*, electron microscopic sections of EMS myosheets failed to reveal any suggestion of myofibrillar thick or thin filaments, Z-bands, or other structural evidence of either forming or degenerating myofibrillar components. The total absence of myofibrillar remnants in EMS myosheets contrasts with the persistence of myofibrillar debris after the disruptive effects of the co-carcinogen 12-*O*-tetradecanoyl phorbol-13-acetate on day 4 myofibrils (9, 12, 13, 35). Wholly unexpected was the voluminous and widespread distribution of SR and T-system elements in these myosheets (Fig. 6*b*). Though EMS blocks the assembly of myofibrils, it did not block the synthesis or assembly of desmin intermediate filaments or the assembly of SR and T-system elements. Details regarding the assembly and distribution of SR-complexes, T-system, intermediate filaments, and microtubules in the total absence of myofibrils will be reported elsewhere.

Immunofluorescence Studies of EMS Myosheets Recovering in Normal Medium

To relate the earliest sites of myofibrillogenesis during recovery to the prominent and extensive SFLS seen in EMS myosheets, we used the double-label immunofluorescence technique. After 3 d in normal medium there was little change in

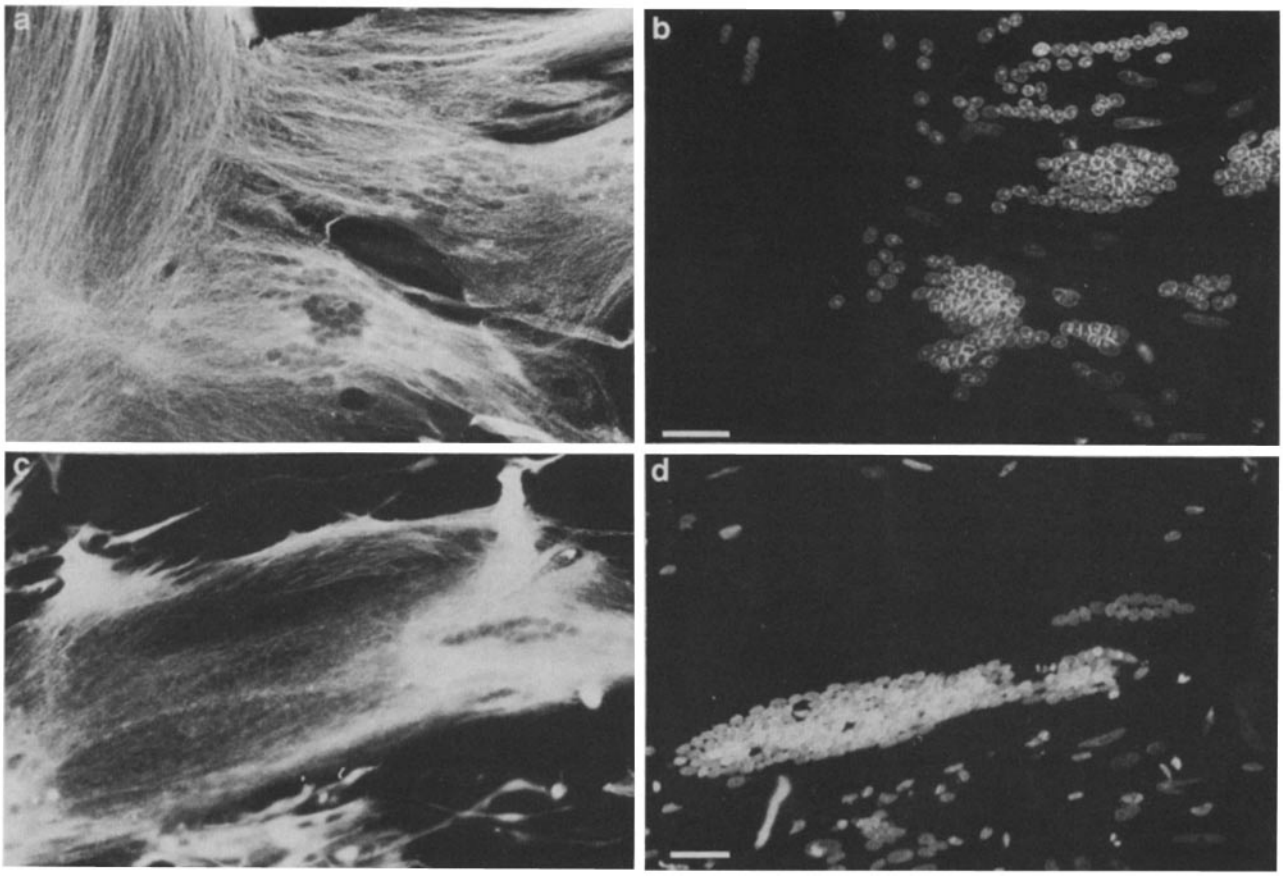

Figure 5. (*a* and *b*) Immunofluorescence micrographs of the same microscopic fields showing antitubulin binding (*a*) using filters to visualize rhodamine, and anti-MS LMM plus a bisbenzimide nuclear stain (*b*) using filters to visualize fluorescein. The long wavy microtubules in *a* tend to run parallel to the long axis of the myosheets. Note in *b* the failure of any structure in these myosheets to bind anti-MS LMM, and the large areas of cytoplasm that are devoid of nuclei. Bar, 50 μm. (*c* and *d*) A portion of the same EMS myosheet visualizing antivimentin (*c*) using rhodamine filters, and anti-MS LMM plus bisbenzimide nuclear stain using fluorescein filters (*d*). Bar, 50 μm.

the morphology of the EMS myosheets. Their prominent SFLS stained positive with anti-CBM, anti-alpha-actinin, and Rho-phalloidin but did not bind either anti-MS LMM or anti-MHC. Binding of the myofibrillar antimyosins was not detected until days 3–4 of recovery. Both myofibrillar myosin antibodies first localized to fine, nonstriated filaments that varied from several hundred to over a thousand microns in length. A single myosheet, depending on its width, could display anywhere from 20 to 80 such well-separated, nonstriated fluorescent filaments. Double staining proved that without exception each myofibrillar myosin positive filament also had properties of a SFLS. These myosin positive nonstriated filaments were similar to those observed at the ends of elongating myofibrils in the growth tips of normal rat (18) and chick myotubes (30, 31, 36).

Double-staining experiments revealed two subsets of filaments in early recovering myosheets. During day 3 of recovery ~80% stained only as SFLS and 20% stained as both SFLS and nascent myofibrils. During the next 24 h, anti-MS LMM staining became co-extensive over most of the length of SFLS that concurrently bound anti-CBM (Fig. 7, *a–d*). By day 5 of recovery, the earlier staining ratios had reversed. During this period, a single fiber staining throughout its length with anti-MS LMM would stain only intermittently with anti-CBM. The emergence of the definitive striated pattern was evident by this time and was accompanied by a gradual loss of filaments that stained with anti-CBM (Fig. 8). Occasionally, nonstriated emerging myofibrils were found alongside definitively striated myofibrils within a single myosheet. The complementary localization of the muscle and nonmuscle myosin isoforms in different myofibrils in these instances was striking (Fig. 9). After 6 d of recovery the anti-CBM failed to stain any longitudinal fibers in the body of the myosheet but was localized henceforth to growth tips and pseudopodial extensions.

The transition of SFLS to striated myofibrils in recovering myosheets was also followed by using various combinations of staining with anti-alpha-actinin and Rho-phalloidin. The average sharp periodicity of a myofibril stained with anti-alpha-actinin (2.3–2.7 μm) was readily distinguished from the irregular periodicity of SFLS (0.6–1.3 μm) stained with the same reagent (compare Fig. 3*d* with 4*f*). Similarly, the complex periodicities displayed by myofibrils after staining with Rho-phalloidin differed greatly from the uniform staining of SFLS by this reagent (compare Fig. 3*c* with 4*e*). During the early recovery period (i.e., days 3–4), double label immunofluorescence experiments with Rho-phalloidin, anti-alpha-actinin, or with antibodies to the muscle-specific myosins resulted in co-localization along preexisting SFLS. After day 5 of recovery the antibodies to alpha-actinin (Fig. 10*a*) or Rho-

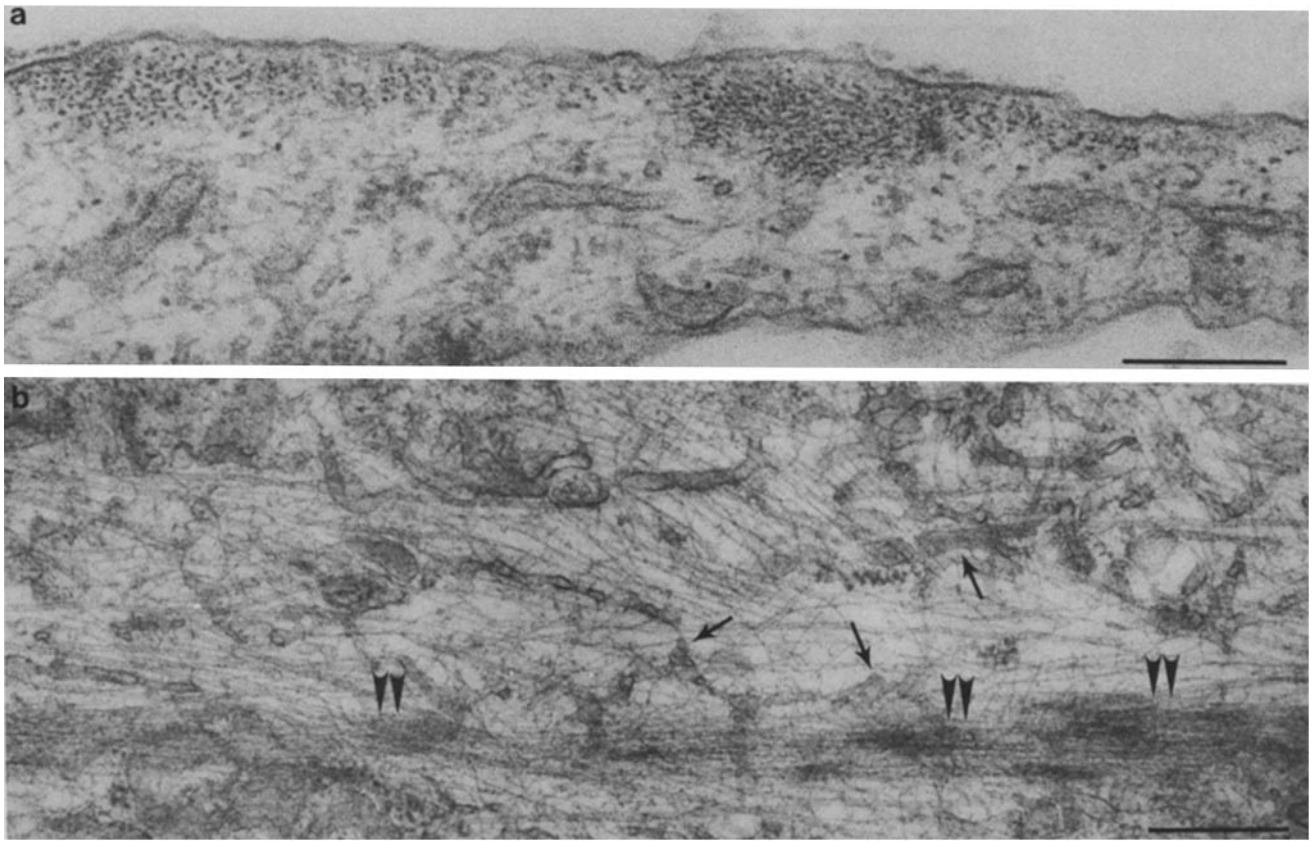

Figure 6. Electron micrographs of day 4 myosheets treated with EMS for the previous 3 d. (*a*) A myosheet viewed in cross-section showing SFLS subtending the upper plasma membrane. (*b*) A longitudinal section showing the extensive SR and T-systems present in EMS myosheets (single arrows). Double arrowheads point to a SFLS. Note the large number of IFs and microtubules in this section. Bars, 0.4 μm.

phalloidin (Fig. 10*c*) stained the numerous well separated fibers with a periodicity identical to that of definitively striated myofibrils. By day 6 of recovery these fluorescent reagents no longer stained SFLS in the body of the recovering myosheets. The remaining small SFLS were confined to the myosheets' growth tips. SFLS that had been so prominent 2–3 d earlier literally disappeared.

Vimentin and desmin intermediate filaments ran largely parallel to and between the emerging myofibrils in normal immature myotubes (5, 24). Only after the formation of A-, I-, Z-, M- and H-bands in sizeable myofibrils did antidesmin localize to the I-Z-region (5, 24, 32–36, 64–66). This shift in the orientation of desmin also occurred in recovering myosheets (data not shown). Between days 4 and 7 of recovery, antivimentin and antidesmin bound to longitudinally oriented filaments only. Thereafter antidesmin could be bound by both longitudinal filaments and transverse structures (compare Fig. 3 in reference 5).

EMS myosheets that were allowed to recover in normal medium for 1–8 d were also stained with antitubulin (data not shown). During this entire recovery period we failed to detect any obvious morphological relationship between microtubules, SFLS, and emerging myofibrils. The polyclonal tubulin antibody used in this study frequently stained microtubule organizing centers in the fibroblastic cells in both normal and EMS-treated cultures. There was no suggestion of such structures in day 4 and older normal myotubes or in the recovering EMS myosheets.

Electron Microscopic Studies of Myosheets Recovering in Normal Medium

Electron microscopic sections confirmed the impression derived from the immunofluorescence studies regarding the proximity of SFLS to the earliest assembly of myofibrillar thick filaments. Myofibrillar thick filaments were never observed in the myosheets while exposed to EMS (Fig. 6) or during the first 2 d of recovery. Only after 3–4 d in normal medium were small numbers of individual thick filaments first identified (Figs. 11, *a* and *b* and 12*a*). These first small aggregates of poorly aligned thick filaments emerged only in association with submembranous SFLS. Thick filaments were not observed without accompanying "thin filaments," or displaced further from the plasma membrane than is shown in Fig. 11*b*. Intermediate filaments and microtubules were often present below, between, and more rarely above, the transitory SFLS-myofibril structures. These electron microscopic findings, coupled with the immunofluorescence data, suggested that during recovery the assembly of muscle-specific myosin and actin monomers into their respective thick and thin filaments was not an event that occurred throughout the sarcoplasm but that was confined to limited domains within the cells, and that these domains included at least one subsarcolemmal SFLS.

By day 5 of recovery, numerous bundles of 50–100 interdigitating thick and thin filaments were observed. Many such bundles were displaced from the sarcolemma by distances of up to 0.5 μm and were organized into sarcomeres containing

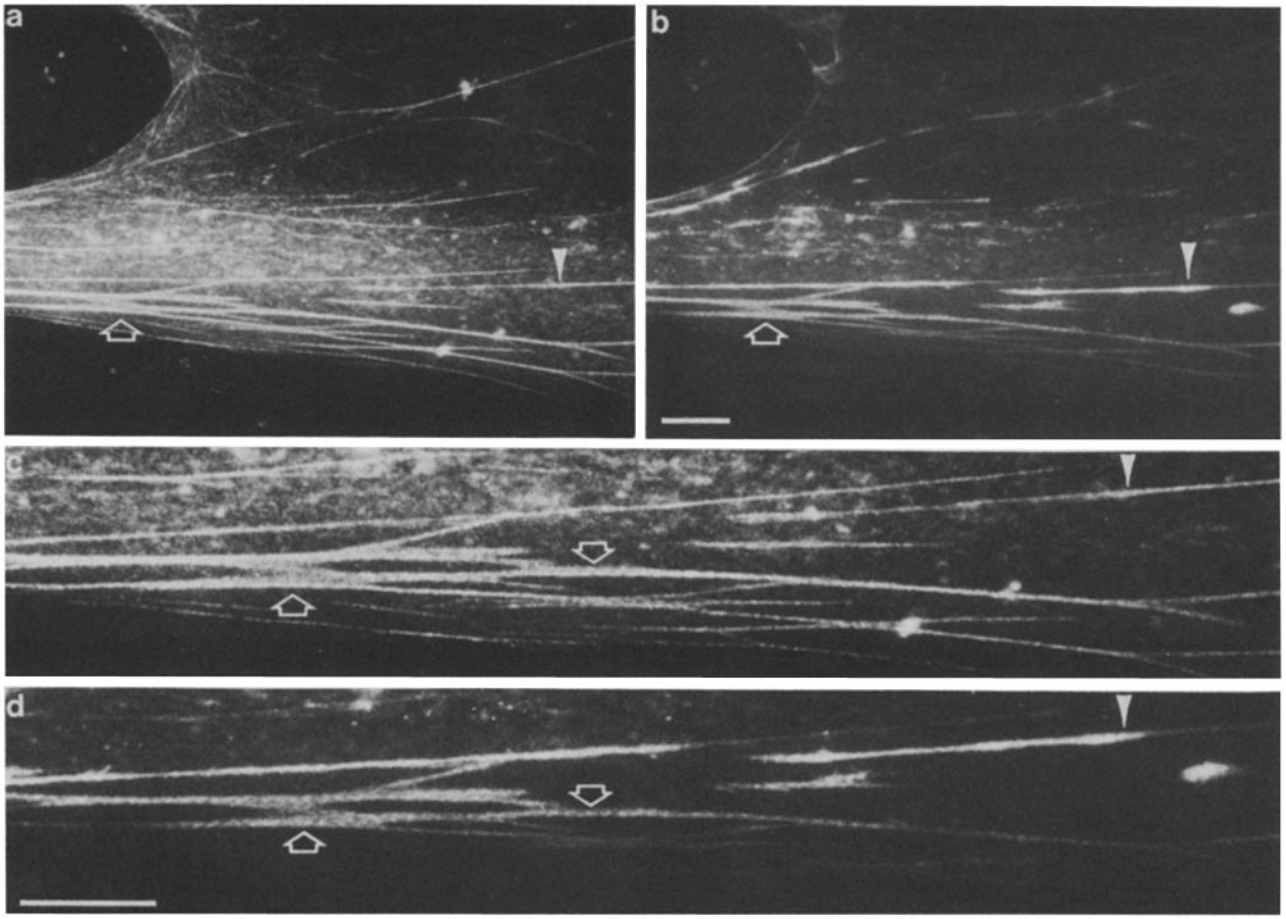

Figure 7. Double label immunofluorescence micrographs showing part of an EMS myosheet after 4 d of recovery. (*a* and *b*) The same microscopic field stained indirectly with anti-CBM (*a*) and directly with FITC-anti-MS LMM (*b*). At this intermediate stage of myofibrillogenesis, the staining patterns along SFLS of these antibodies to nonmuscle (*a*) and muscle myosin (*b*) isoforms are largely co-extensive. Arrows and arrowheads point to representative areas of co-extensive staining. (*c* and *d*) At higher magnification, part of the microscopic field shown in *a* and *b*. Bars, 20 μm.

distinct A-, I-, and Z-bands (Figs. 11*c* and 12*b*). The thin well-separated myofibrils often branched and interconnected with one another, mirroring the branches and interconnections observed with the earlier SFLS. The small SFLS that remained were strictly confined to the growth tips and to the flattened pseudopodial processes. If maintained in normal medium for another 4 or 5 d, the number and width of the myofibrils increased greatly and came to occupy most of the interior of the sarcoplasm. Note in Fig. 12*b* the numerous longitudinally deployed intermediate filaments; note, too, the absence of any obvious association of the intermediate filaments with the well-formed Z-bands. Similarly, microtubules were always observed in the vicinity of the emerging and maturing myofibrils. But again, with our techniques no consistent obvious morphological links between microtubules and other fibrous elements were noted. On the other hand, low-magnification surveys revealed a striking aggregation of SR elements at the level of I-Z-band in nascent myofibrils. The possible role of this periodic arrangement of SR in aligning individual myofibrils will be described elsewhere.

Immunoblot Analysis of Cultures in, and Recovering from, EMS

The cytoimmunofluorescence and electron microscopic data showed that myosheets did not assemble myofibrillar isoforms into nascent myofibrils even if allowed to recover in normal medium for 2 d. Myofibrillar structures were not detected in recovering myosheets until days 3–4 of recovery. In addition, the microscopic data suggested that before recovery, SFLS that bind anti-CBM were abundant in EMS myosheets, whereas after recovery the SFLS disappear. Both of these conclusions were verified by performing immunoblots on whole cell lysates of these cultures. Samples from EMS-treated cultures not allowed to recover failed to bind the anti-MS LMM (Fig. 13*B*, lane *2*). Conversely, samples from the EMS cultures bound more anti-CBM per microgram DNA (Fig. 13*C*, lane 2) than samples from either control or EMS-recovered cultures (Fig. 13*C*, lanes *1* and *3*). As shown in Fig. 13*B*, lanes *1* and *3*, samples from both day 4 control and EMS-treated cultures allowed to recover for 4 d strongly bound the anti-MS LMM.

The failure of anti-CBM to recognize the muscle myosin isoform was demonstrated by performing immunoblots of glycerinated chicken myofibrils. When preparations of myofibrils were displayed by gel electrophoresis (Fig. 13*d*, lane *1*) and transferred to nitrocellulose, the transfers failed to bind anti-CBM (Fig. 13*D*, lane *2*).

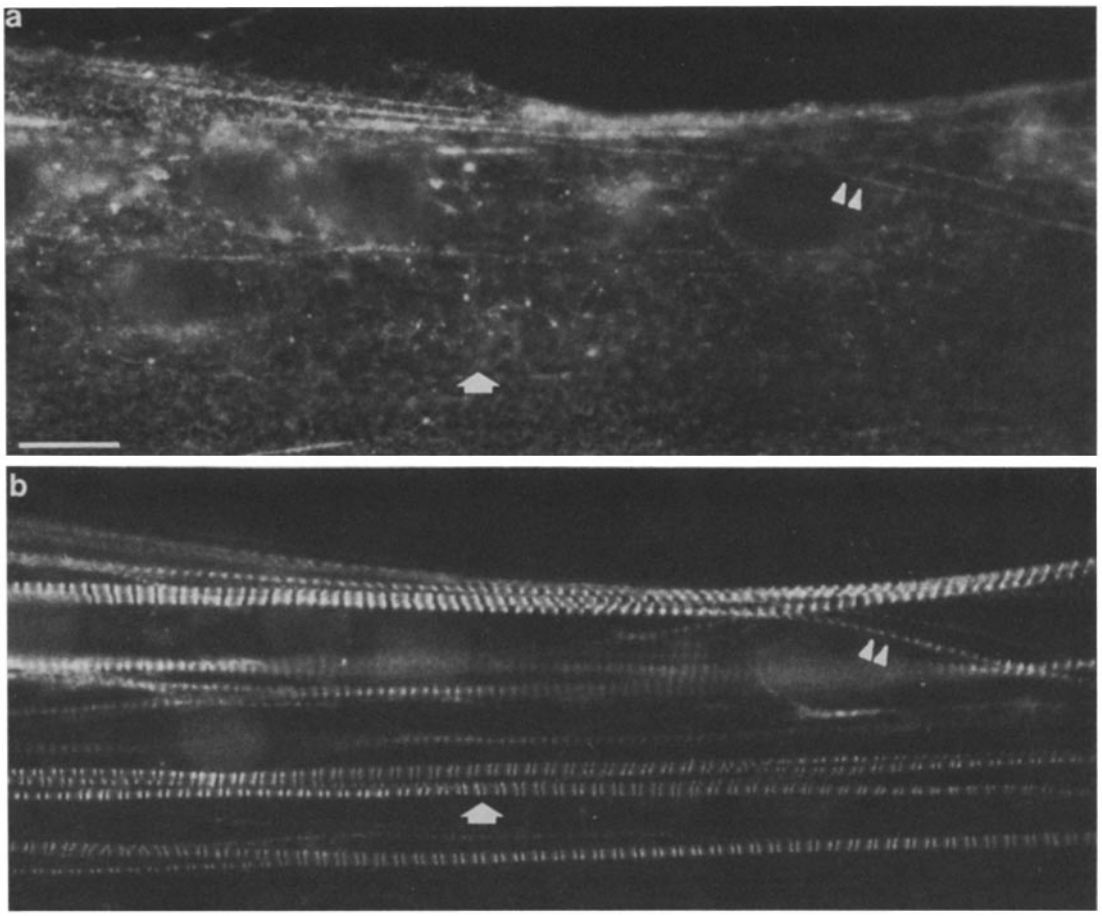

Figure 8. (*a* and *b*) Double label immunofluorescence micrographs of the same microscopic field showing a small portion of an EMS myosheet after 5 d of recovery. The myosheet is stained with both indirectly labeled anti-CBM (*a*) and directly labeled FITC-anti-MS LMM (*b*). Anti-MS LMM binds to the lateral edges of each A-band (*b*) and shows distinct myofibrils exhibiting well-ordered sarcomeres ~2.3 μm long. The emergence of definitive myofibrils is accompanied by the loss of co-extensive anti-CBM staining (*a*) (arrows). Occasionally, very fine myofibrils showing sarcomeric anti-MS LMM staining will stain co-extensively with anti-CBM (double arrowheads). Bar, 10 μm.

Discussion

EMS is an ultimate carcinogen. It has been used to mutagenize cultured myogenic cells (48) and to generate mutant genes coding for myosin heavy chains (17). We used a concentration of EMS that permits fusion of postmitotic myoblasts into multinucleated myosheets but is toxic to both replicating fibroblasts and presumptive myoblasts. These cultures are ideal for combined cytoimmunofluorescence, electron microscopic, and biochemical studies owing to the reduction of contaminating mononucleated cells, the unusually flattened condition of the myosheets, and the long period required for completion of the earliest phases of myofibrillogenesis after the shift of EMS myosheets to normal medium (1, 34, 35).

The immunofluorescence and electron microscopic observations reported here on nascent myofibril formation in recovering EMS myosheets support the conclusion that the earliest assembly of muscle-specific thick and thin filaments is an event that does not occur randomly throughout the cytoplasm but is strictly confined to certain longitudinal microdomains within the muscle cells. Previous observations on the origin of myofibrils have suggested a submembranous "birthplace" (21, 29–31, 36, 38); our evidence links this to the existence of SFLS in this location. The co-linearity of virtually all nascent myofibrils with preexisting SFLS suggests either that the latter system determines the longitudinal microdomain in which the newly polymerized thick and thin filaments are first assembled into striated myofibrils, or that the sharply defined longitudinal microdomains of both nascent myofibrils and SFLS are determined by still other unknown system(s) associated with the cells' cortex. This might involve participation of subcortical cytoskeletal elements interacting with integral or peripheral membrane proteins.

The role of vinculin and spectrin in attaching stress fibers to the inner face of the plasma membrane has been emphasized (47, 51). The failure of antivinculin and antispectrin to stain the great majority of myofibrils suggests that these molecules are not permanent structures in all myofibrils but may serve to link mechanically the peripheral myofibrils to the sarcolemma during contraction. Nevertheless, one or both molecules may be associated with nascent myofibrils and be lost subsequently as the myofibrils mature and are displaced from the cells' periphery, remaining only with the final group of submembranous myofibrils.

The gradual emergence of a striated myofibril in recovering EMS myosheets must involve a complex molecular transition between a given SFLS and a given myofibril. At the earliest stages, myofibrils may be either true hybrid structures of both

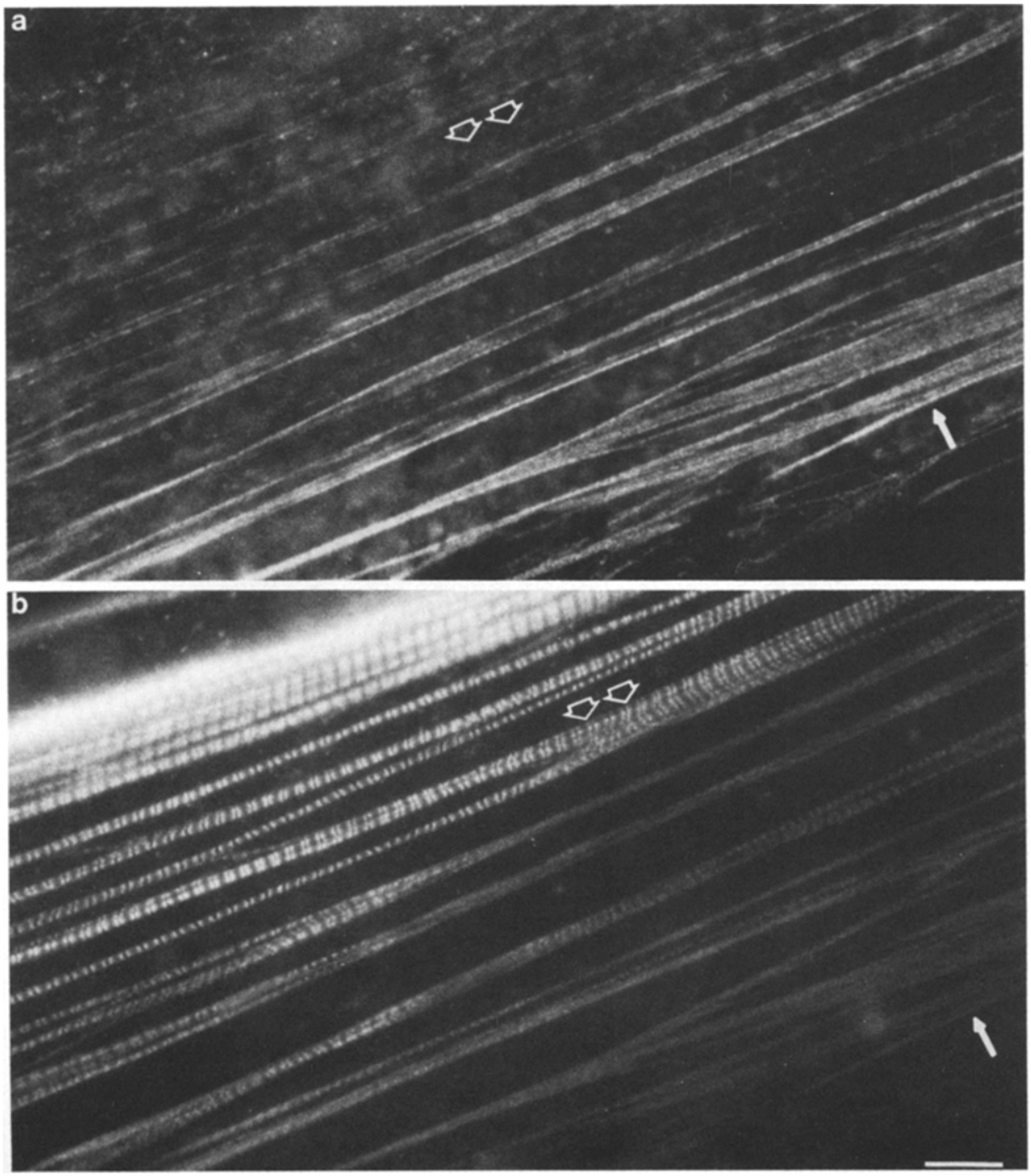

Figure 9. Double label immunofluorescence micrographs showing the same microscopic field of a small portion of a recovering EMS myosheet visualized with both indirectly labeled rhodamine-anti-CBM (*a*) and directly labeled FITC-anti-MS LMM (*b*). Myofibrils at various stages of maturation are visible in this microscopic field. The complementary localization of the nonmuscle (*a*) and muscle (*b*) myosin isoforms is striking. At the lower right of the micrographs, anti-MS LMM co-localizes along SFLS that stain prominently with anti-CBM (*a* and *b*, single arrows). Towards the upper left of the micrographs, anti-MS LMM shows sarcomeric staining patterns, and anti-CBM staining, indicative of SFLS, has disappeared (*a* and *b*, double arrows). Bar, 10 μm.

myofibrillar and constitutive contractile protein isoforms, or two distinct but juxtaposed structures. With our techniques, we could not determine whether the earliest muscle-specific myosin heavy chains and alpha-actin monomers form transitory heteropolymers with the cytoplasmic myosin and beta- and gamma-actins of SFLS, or whether they directly assemble into homopolymers of myofibrillar thick and thin filaments in the vicinity of the pre-existing SFLS. It is interesting that 10 min after microinjection, actin isolated from skeletal muscle localizes to stress fibers of fibroblasts (26). Similarly, transfection of an alpha-actin gene sequence into fibroblasts showed that the alpha-actin protein can interact with the fibroblasts' cytoskeleton (28). Myosin filaments that are heteropolymers of muscle-specific and cytoplasmic myosin monomers have also been reported to assemble in vitro (55).

Individual, striated myofibrils are often most easily visualized in the vicinity of nuclei both in postmitotic mononucleated myoblasts and in myotubes (29–33), but this may only reflect the larger amount of sarcoplasm in the perinuclear regions. EMS myosheets contained large areas of cytoplasm that lack nuclei (Figs. 1, 4, and 5). If there was any consistent correlation between areas rich in nuclei and the sites of

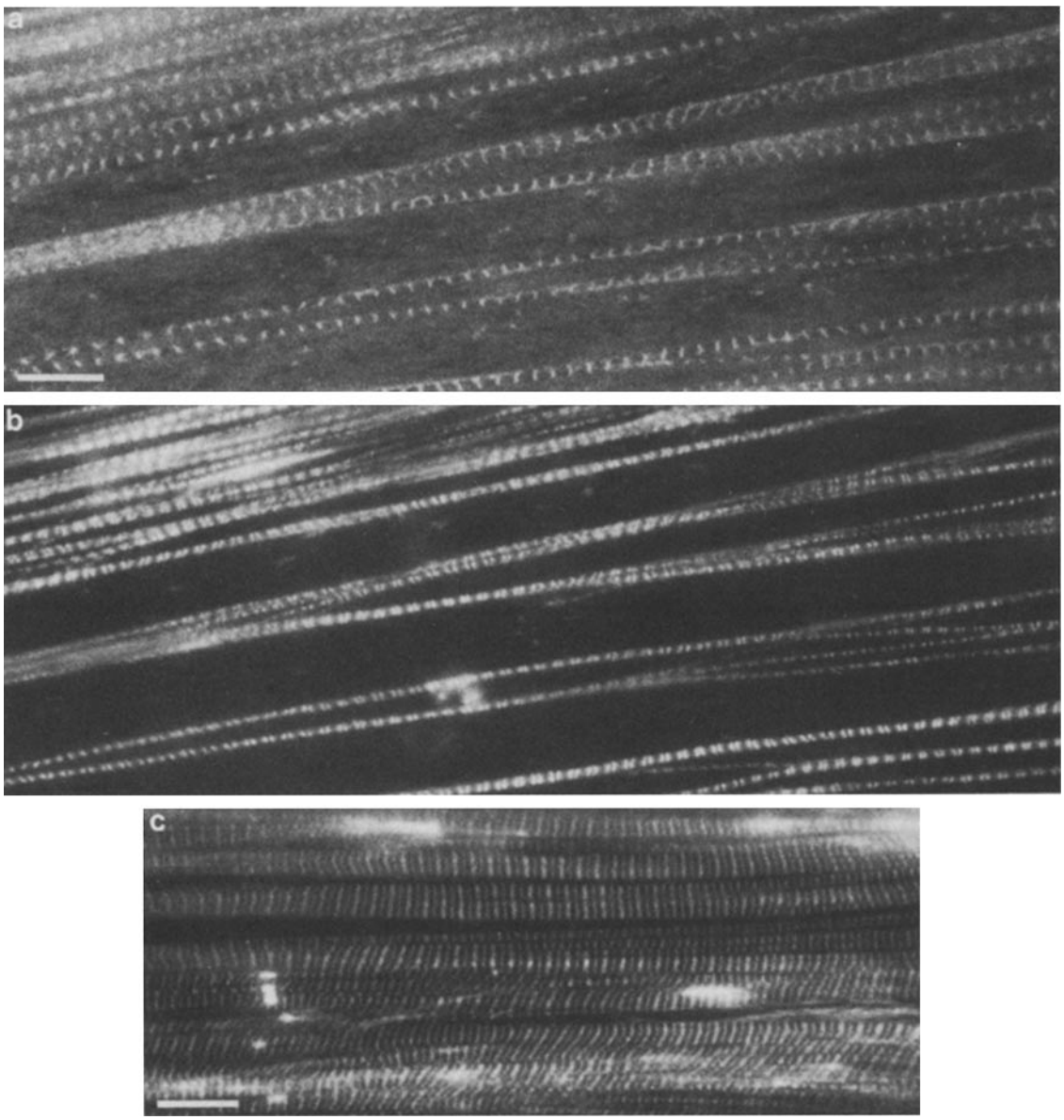

Figure 10. (*a* and *b*) Immunofluorescence micrographs of the same microscopic field showing a portion of an EMS myosheet after 5 d of recovery. At this late stage of recovery, anti-alpha actinin (*a*) binds in a distinct 2.3–2.5-μm banding pattern characteristic of Z-band staining of definitive myofibrils. Anti-MS LMM (*b*) binds to the lateral portions of each A-band in these striated myofibrils. (*c*) A small portion of an EMS myosheet after 5 d of recovery, stained with Rho-phalloidin to visualize actin. This unusual banding pattern was also obtained with glycerinated myofibrils and varied depending upon the extent of myofibril contraction. Note the total absence of SFLS at this relatively late stage of recovery. Bars, 10 μm.

emergence of nascent myofibrils, it escaped our detection. We were also impressed with the relatively constant width, often for distances >0.2 mm, of individual myofibrils in recovering myosheets. Uniform width was characteristic of not only nascent myofibrils but also of myofibrils in myosheets that had recovered for >8 d. If the density of mRNAs coding for the myofibrillar isoforms fell off with distance from the nuclei, this gradient was not reflected in the gross morphology or distribution of the emerging myofibrils. It will be interesting to determine by in situ hybridization the distribution of mRNAs coding for the myofibrillar isoforms in these myosheets.

We tried to detect reproducibly longitudinally aligned sarcomeric structures with a measured repeat smaller than that observed in fully assembled myofibrils in control cultures. In all instances, as soon as a periodic staining pattern was detected with either anti-LMM or anti-MHC, it invariably involved a repeat pattern of a size observed in mature myofibrils. Double staining of such myofibrillar myosin-positive fibrils with anti-alpha-actinin revealed a repeat pattern of the latter in the same size range. These observations do not support the notion that there is a gradual and systematic transition from mini to definitive length sarcomeres during myofibrillogenesis, at least in our preparations.

Our findings suggest that the formation and maturation of a given myofibril requires passage through several distinct phases (see reference 14). The first phase involves the earliest assembly of poorly aligned thick and thin filaments into

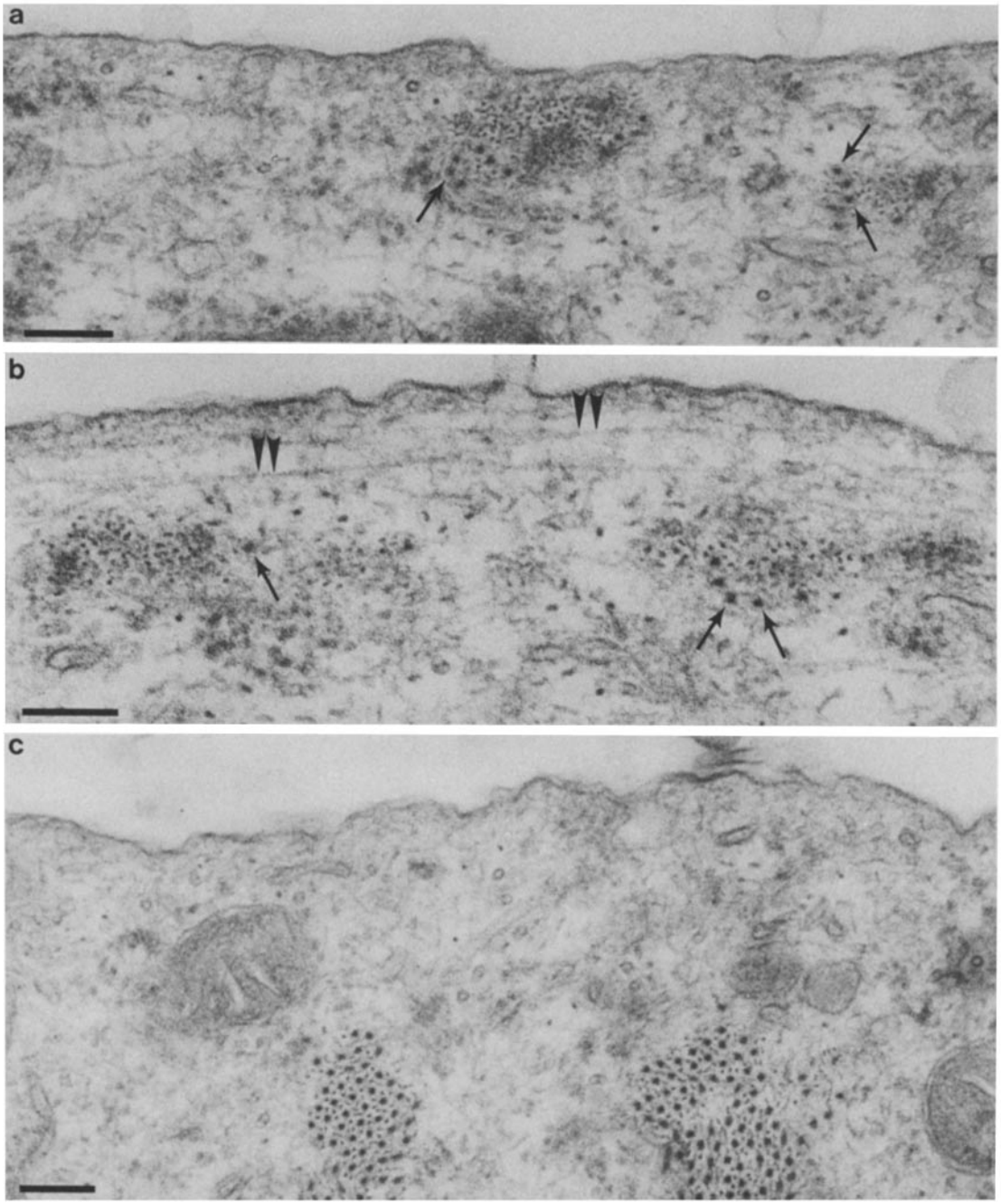

Figure 11. Electron micrographs showing cross-sections of myosheets during various stages of recovery from exposure to EMS. When the earliest immunofluorescence staining with anti-MS LMM or anti-MHC is observed in recovering myosheets, cross-sections reveal myosin filament profiles in close association with SFLS (*a* and *b*, arrows). Usually, myosin filaments are located around the periphery, or interspersed with a few of the thin filaments associated with the SFLS. Double arrowheads in *b* point to transversely oriented intermediate filaments. SFLS with associated myofibrillar myosin filaments are rapidly displaced from the plasma membrane, where emerging myofibrils increase in diameter by the addition of thick and thin filaments. Soon after displacement from the plasmalemma, thick and thin filaments begin to take on the hexagonal stacking pattern characteristic of well-ordered, striated myofibrils (*c*). Bars, 0.5 μm.

rudimentary striated myofibrils, each of which forms near an individual submembranous SFLS. Subsequent phases involve (*a*) the more rigorous lateral alignment of individual filaments into a lattice of hexagonally stacked interdigitating thick and thin filaments; (*b*) the uniform growth in diameter along the length of the myofibril by the precise apposition of newly polymerized thick and thin filaments into their appropriate subdivision of full length sarcomeres (i.e., A- and I-bands); (*c*) the addition in the cell's growth tips of newly assembled, full length sarcomeres at the ends of individual myofibrils; and (*d*) the displacement of individual myofibrils into the sarcoplasm (30, 36, 49). Whether all myofibrils can be traced to a submembranous birthplace or whether during maturation and/or regeneration pre-existing myofibrils increase in number by splitting remains to be determined.

The precise temporal relationships between the displace-

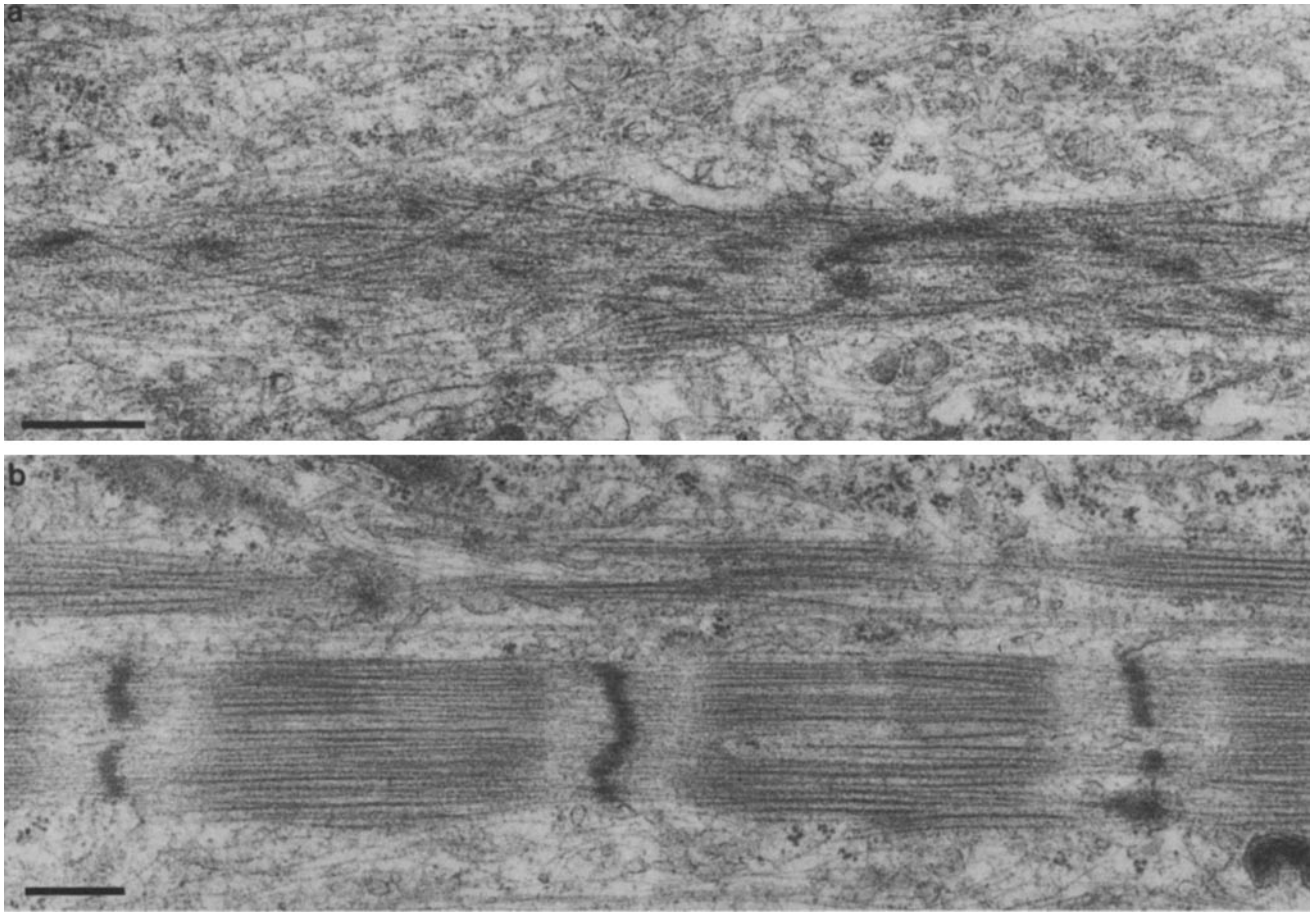

Figure 12. Electron micrographs showing longitudinal sections of myosheets during recovery from EMS exposure. At intermediate times of recovery, emerging myofibrils exhibit poorly aligned thick filaments interspersed with patches of electron dense, Z-band-like material (*a*). Actin filaments are often visible emanating from these electron dense patches. (*b*) Example of a well-ordered myofibril typical of the large number visible in recovering EMS myosheets after 6 d in normal medium. Note the predominantly longitudinal arrangement of the intermediate filaments. Typical A-, I-, and Z-bands are visible, as are the SR and T tubule systems. Bars, 0.5 μm.

ment from the plasma membrane and the disappearance of SFLS is unclear. Evidently myogenic cells contain mechanisms for the segregation of a group of isoforms and for their separate, but related, assembly, and other mechanisms for subsequent degradation of one set. This suggests that the program for myofibrillogenesis is more complex than the mere initiation of transcription of a group of muscle-specific genes, however coordinate. The complete program must also contain specification for the removal of the earliest structures involved in the assembly of the nascent myofibril. This could occur via normal protein turnover following the down-regulation of the genes coding for the appropriate nonmuscle contractile proteins, via selective protein degradation, or by a combination of these processes (3). Many functions have been attributed to stress fibers in various kinds of cells. It is of considerable theoretical interest that they are lost early during myotube maturation.

With these results on recovering EMS myosheets in mind, we reexamined myofibril formation in normally developing chick myotubes. Preliminary experiments show a similar co-distribution of muscle and nonmuscle myosins in day 3 myotubes. Anti-CBM staining frequently co-localizes along fibrillar structues that stain continuously with anti-MS LMM. This is particularly evident along the outer curvature of arcing myotubes where they often spread and flatten, and in the myotube's growth tips. In areas where anti-MS LMM staining is organized into well-ordered striations, anti-CBM staining shows only a diffuse cytoplasmic fluorescence (Fig. 3, *a* and *b*), in agreement with previous studies (14, 18). A more detailed examination of myofibrillogenesis in normal developing myotubes using anti-MS LMM and anti-CBM will be presented elsewhere.

Throughout this work we deliberately searched for obvious morphological relationships between intermediate filaments or microtubules and either the transitory SFLS or the emerging myofibrils. The fact that we did not find any does not mean that none exists. During myofibrillogenesis there is a dramatic shift from a predominantly longitudinal distribution of desmin to a predominantly transverse distribution. However, this redistribution occurs several days after the formation of definitive Z-bands, and we find no evidence that desmin links nascent myofibrils to the plasma membrane (5, 32–36, 64–66). The striking effects of colcemid and taxol on myofibrillogenesis suggest major roles for both intermediate filaments and microtubules in the structuring of nascent myofibrils (1, 2, 11, 32, 35, 67). However, our observations indicate a close structural relationship between transitory SFLS and myofibrils and suggest that this is more direct than the poten-

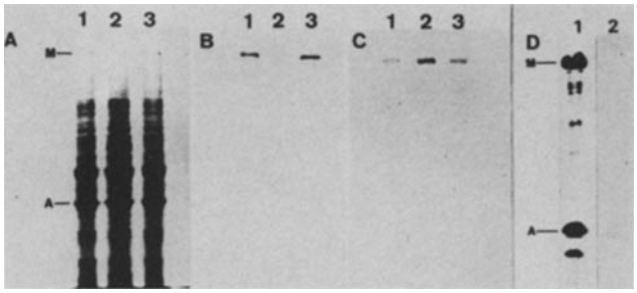

Figure 13. Immunoblot analysis of Triton X-100-insoluble proteins from day 4 control cultures (*A–C*, lane *1*), day 4 cultures exposed to EMS for the previous 3 d (*A–C*, lane *2*), and day 4 cultures exposed to EMS for the previous 3 d and then allowed to recover in normal medium for 4 d (*A–C*, lane *3*). Sample loads were standardized to 0.5 μg DNA. Whole cell homogenates from the three groups were electrophoresed on a 10% SDS gel (*A*) and then electrophoretically transferred to nitrocellulose filters for 48 h (*B* and *C*). *A* shows a replica gel stained with Coomassie Blue. The transfers to nitrocellulose were incubated with anti-MS LMM (*B*) and with anti-CBM (*C*). The bound antibodies were visualized by the peroxidase-anti-peroxidase technique of Sternberger (61). To confirm the specificity of anti-CBM, homogenates of glycerinated chick myofibrils were displayed by SDS PAGE (*D*, lane *1*), transferred to nitrocellulose, and incubated with anti-CBM (*D*, lane *2*). Binding of anti-CBM to the skeletal muscle myosin isoform was not detectable. *M*, myosin heavy chain; *A*, actin.

tial contributions of microtubules or intermediate filaments to myofibrillogenesis.

We acknowledge the assistance of Joshua Kavaler and Christopher J. Jones in preparing the antibody against CBM.

This work was supported by National Institutes of Health grants CA-18194, HD-07512, HL-18708, and HL-15835 (to the Pennsylvania Muscle Institute) and the Muscular Dystrophy Association. P. B. Antin is the recipient of a Revson-Winston Fellowship from Cornell University Medical College.

Received for publication 9 August 1985, and in revised form 12 November 1985.

References

1. Antin, P. B., S. Forry-Schaudies, S. Duran, J. Eshleman, and H. Holtzer. 1985. Using a co-carcinogen (TPA) and a carcinogen (EMS) to probe myofibrillogenesis. *UCLA Symp. (Univ. Calif. Los Ang.)* Symp. Mol. Cell. Biol. New Ser. 29. In press.

2. Antin, P., S. Forry-Schaudies, T. Friedman, S. Tapscott, and H. Holtzer. 1981. Taxol induces postmitotic myoblasts to assemble interdigitating microtubule-myosin arrays that exclude actin filaments. *J. Cell Biol.* 90:300–308.

3. Bandman, E., and R. Strohman. 1982. Increased K^+ inhibits spontaneous contractions and reduces myosin accumulation in cultured chick myotubes. *J. Cell Biol.* 93:698–704.

4. Bennett, G. S., S. A. Fellini, and H. Holtzer. 1978. Immunofluorescent visualization of 100 A filaments in different cultured chick embryonic cell types. *Differentiation.* 12:71–82.

5. Bennett, G. S., S. Fellini, Y. Toyama, and H. Holtzer. 1979. Redistribution of intermediate filament subunits during skeletal myogenesis and maturation in vitro. *J. Cell Biol.* 82:577–584.

6. Berner, P., E. Frank, H. Holtzer, and A. P. Somlyo. 1981. The intermediate filament proteins of rabbit vascular smooth muscle: immunofluorescent studies of desmin and vimentin. *J. Muscle Res. Cell Motil.* 2:439–452.

7. Bischoff, R., and H. Holtzer. 1967. The effect of mitotic inhibitors on myogenesis in vitro. *J. Cell Biol.* 36:111–128.

8. Chi, J. C., S. A. Fellini, and H. Holtzer. 1975. Differences among myosins synthesized in non-myogenic cells, presumptive myoblasts and myoblasts. *Proc. Natl. Acad. Sci. USA.* 72:4999–5003.

9. Cohen, R., M. Pacifici, N. Rubinstein, J. Biehl, and H. Holtzer. 1977. Effects of a tumor promoter (PMA) on myogenesis. *Nature (Lond.).* 266:538–540.

10. Craig, S. W., and T. V. Pardo. 1979. Alpha-actinin localization in the junctional complex of intestinal epithelial cells. *J. Cell Biol.* 80:203–210.

11. Croop, J. M., and H. Holtzer. 1975. Response of fibrogenic and myogenic cells to cytochalasin B and to colcemid. I. Light microscopic observations. *J. Cell Biol.* 65:271–285.

12. Croop, J., G. Dubyak, Y. Toyama, A. Dlugosz, A. Scarpa, and H. Holtzer. 1982. Effects of 12-O-tetradecanoyl-phorbol-13-acetate on myofibril integrity and Ca^{++} content in developing myotubes. *Dev. Biol.* 89:460–474.

13. Croop, J. M., Y. Toyama, A. Dlugosz, and H. Holtzer. 1980. Selective effects of phorbol-12-myristate-13 acetate on myofibrils and 10 nm filaments. *Proc. Natl. Acad. Sci. USA.* 77:5273–5277.

14. Dlugosz, A. A., P. B. Antin, V. T. Nachmias, and H. Holtzer. 1984. The relationship between stress fiber-like structures and nascent myofibrils in cultured cardiac myocytes. *J. Cell Biol.* 99:2268–2278.

15. Dlugosz, A. A., S. J. Tapscott, and H. Holtzer. 1983. Effects of phorbol 12-myristate 13-acetate on the differentiation program of embryonic chick skeletal myoblasts. *Cancer Res.* 43:2780–2789.

16. Endo, T., and T. Masaki. 1984. Differential expression and distribution of chicken skeletal- and smooth-muscle-type alpha-actinins during myogenesis in culture. *J. Cell Biol.* 99:2322–2332.

17. Epstein, H. F., R. H. Waterston, and S. Brenner. 1974. A mutant affecting the heavy chain of myosin in *Caenorhabditis elegans. J. Mol. Biol.* 90:291–300.

18. Fallon, J. R., and V. T. Nachmias. 1980. Localization of cytoplasmic and skeletal myosins in developing muscle cells by double-label immunofluorescence. *J. Cell Biol.* 87:237–247.

19. Fellini, S., G. Bennett, and H. Holtzer. 1978. Selective binding of antibody against 10 nm filaments to different cell types in myogenic cultures. *Am. J. Anat.* 153:451–457.

20. Feramisco, J. 1979. Microinjection of fluorescently labelled alpha-actinin in living fibroblasts. *Proc. Natl. Acad. Sci. USA.* 76:3967–3971.

21. Fischman, D. A. 1970. The synthesis and assembly of myofibrils in embryonic muscles. *Curr. Top. Dev. Biol.* 5:235–280.

22. Fischman, D. A. 1972. Development of striated muscle. *In* The Structure and Function of Muscle, 2nd edition, Volume 1. G. H. Bourne, editor. Academic Press, New York. 75–148.

23. Fujiwara, K., and T. Pollard. 1976. Fluorescent antibody localization of myosin in the cytoplasm, cleavage furrow, and mitotic spindle of human cells. *J. Cell Biol.* 71:848–875.

24. Gard, D., and E. Lazarides. 1980. The synthesis and distribution of desmin and vimentin during myogenesis *in vitro. Cell.* 19:263–275.

25. Geisler, N., and K. Weber. 1981. Comparison of two immunologically distinct intermediate-sized filaments by amino acid sequence analysis: desmin and vimentin. *Proc. Natl. Acad. Sci. USA.* 78:4120–4124.

26. Glacy, S. D. 1983. Subcellular distribution of rhodamine-actin microinjected into fibroblastic cells. *J. Cell Biol.* 97:1207–1213.

27. Gordon, W. E. 1978. Immunofluorescent ultrastructural studies of "sarcomeric" units in stress fibers of cultured non-muscle cells. *Exp. Cell Res.* 117:253–260.

28. Gunning, P., P. Ponte, L. Kedes, R. J. Hickey, and A. I. Skoultchi. 1984. Expression of human cardiac actin in mouse L cells. A sarcomeric actin associates with a nonmuscle cytoskeleton. *Cell.* 36:709–715.

29. Holtzer, H. 1959. *In* Biological Organization: Cellular and Subcellular. Proceedings of a symposium organized on behalf of UNESCO, held at the University of Edinburgh, Scotland; September, 1957. C. H. Waddington, editor. Pergamon Press, New York. 142–152.

30. Holtzer, H., and J. W. Sanger. 1972. Myogenesis, old views rethought. *In* Research in Muscle Development and the Muscle Spindle. B. Banker, R. Przybylski, J. Vander Moulen, and M. Victor, editors. *Excerpta Med. Int. Congr. Ser.* 122–133.

31. Holtzer, H., J. Marshall, and H. Finck. 1957. An analysis of myogenesis by the use of fluorescent antimyosin. *J. Biophys. Biochem. Cytol.* 8:705–723.

32. Holtzer, H., G. S. Bennett, S. J. Tapscott, J. M. Croop, and Y. Toyama. 1982. Intermediate-sized filaments: changes in synthesis and distribution in cells of myogenic and neurogenic lineages. *Cold Spring Harbor Symp. Quant. Biol.* 46:317–329.

33. Holtzer, H., J. Croop, Y. Toyama, G. Bennett, S. Fellini, and C. West. 1980. Differences in differentiation programs between presumptive myoblasts and their daughters, the definitive myoblasts and myotubes. *In* Plasticity of Muscle. D. Pette, editor. Walter de Gruyter & Co., Berlin. 823–839.

34. Holtzer, H., S. Forry-Schaudies, P. Antin, G. Dubyak, and V. Nachmias. 1985. Induction of incoordinate synthesis of muscle proteins by the tumor promoter TPA and the carcinogen EMS. *In* Gene Expression in Muscle. S. Wolf and R. Strohman, editors. Plenum Press, New York. 129–136.

35. Holtzer, H., S. Forry-Schaudies, A. Dlugosz, P. Antin, and G. Dubyak. 1985. Interactions between IF's, microtubules and myofibrils in fibrogenic and myogenic cells. *In* Intermediate Filaments. *Ann. NY Acad. Sci.* 455:106–125.

36. Holtzer, H., J. Sanger, H. Ishikawa, and K. Strahs. 1972. Selected topics in skeletal myogenesis. *Cold Spring Harbor Symp. Quant. Biol.* 37:549–566.

37. Ishikawa, H., R. Bischoff, and H. Holtzer. 1969. The formation of arrowhead complexes with heavy meromyosin in a variety of cell types. *J. Cell Biol.* 43:312–328.

38. Kelly, D. E. 1969. Myofibrillogenesis and z-band differentiation. *Anat. Rec.* 163:403–426.

39. Kreis, T., and W. Birchmeier. 1980. Stress fiber sarcomeres of fibroblasts are contractile. *Cell.* 22:555–561.

40. Kuczmarski, E. R., and J. L. Rosembaum. 1978. Chick brain actin and

myosin. Isolation and characterization. *J. Cell Biol.* 80:341–355.

41. Kulikowski, R. R., and F. J. Manasek. 1979. Myosin localization in cultured embryonic cardiac myocytes. *In* Motility in Cell Function. F. Pepe, J. Sanger, and V. Nachmias, editors. Academic Press Inc., New York. 433–435.

42. Lazarides, E. 1975. Tropomyosin antibody: the specific localization of tropomyosin in non-muscle cells. *J. Cell Biol.* 65:549–561.

43. Lazarides, E., and K. Weber. 1974. Actin antibody: the specific visualization of actin filaments in non-muscle cells. *Proc. Natl. Acad. Sci. USA.* 71:2268–2273.

44. Lubit, B. W., and J. H. Schwartz. 1980. An anti-actin antibody that distinguishes between cytoplasmic and skeletal muscle actins. *J. Cell Biol.* 87:237–247.

45. Maupin, P., and T. Pollard. 1983. Improved preservation and staining of HeLa cell actin filaments, clathrin-coated membranes, and other cytoplasmic structures by tannic acid-glutarldehyde-saponin fixation. *J. Cell Biol.* 96:51–52.

46. Moss, P., and R. Strohman. 1976. Myosin synthesis by fusion-arrested chick embryo myoblasts in cell culture. *Dev. Biol.* 48:431–437.

47. Nelson, W. J., and E. Lazarides. 1984. Goblin (ankyrin) in striated muscle: identification of the potential membrane receptor for erythroid spectrin in muscle cells. *Proc. Natl. Acad. Sci. USA.* 81:3292–3296.

48. Nguyen, H. T., R. M. Medford, and B. Nadal-Ginard. 1983. Reversibility of muscle differentiation in the absence of commitment: analysis of a myogenic cell line temperature-sensitive for commitment. *Cell.* 34:281–293.

49. Okazaki, K., and H. Holtzer. 1965. An analysis of myogenesis in vitro using fluorescein-labelled antimyosin. *J. Histochem. Cytochem.* 13:726–739.

50. Osborn, M., R. Webster, and K. Weber. 1978. Individual microtubules viewed by immunofluorescence and electron microscopy in the same ptK2 cell. *J. Cell Biol.* 77:R27–R34.

51. Pardo, J. V., J. D. Siliciano, and S. W. Craig. 1983. Vinculin is a component of an extensive network of myofibril-sarcolemma attachment regions in cardiac muscle fibers. *J. Cell Biol.* 97:1081–1088.

52. Pearson, M. L., and H. F. Epstein. 1982. Muscle Development: Molecular and Cellular Control. Cold Spring Harbor Laboratory, Cold Spring Harbor, NY.

53. Peng, H. B., J. J. Wolosewick, and P.-C. Cheng. 1981. The development of myofibrils in cultured muscle cells: a whole mount and thin section electron microscopic study. *Dev. Biol.* 88:121–136.

54. Pollak, R., M. Osborn, and K. Weber. 1975. Patterns of organization of actin and myosin in normal and transformed cultured cells. *Proc. Natl. Acad. Sci. USA.* 72:994–998.

55. Pollard, T. D. 1975. Electron microscopy of synthetic myosin filaments: evidence for cross-bridge flexibility and copolymer formation. *J. Cell Biol.* 67:93–104.

56. Rubinstein, N., J. Chi, and H. Holtzer. 1974. Actin and myosin in a variety of myogenic and non-myogenic cells. *Biochem. Biophys. Res. Commun.* 57:438–443.

57. Rubinstein, N., J. Chi, and H. Holtzer. 1976. Coordinated synthesis and degradation of actin and myosin in a variety of myogenic and non-myogenic cells. *Exp. Cell Res.* 97:387–393.

58. Sanger, J. W., B. Mittal, and J. M. Sanger. 1984. Formation of myofibrils in spreading chick cardiac myocytes. *Cell Motil.* 4:405–416.

59. Sanger, J. W., J. M. Sanger, and B. M. Jockusch. 1983. Differences in the stress fibers between fibroblasts and epithelial cells. *J. Cell Biol.* 96:961–969.

60. Shimada, Y., and T. Obinata. 1977. Polarity of actin filaments at the initial stage of myofibril assembly in myogenic cells in vitro. *J. Cell Biol.* 72:777–785.

61. Sternberger, L. A., P. H. Hardy, J. Cuculis, and H. G. Meyer. 1970. The unlabelled antibody method of immunohistochemistry. Preparation and properties of soluble antigen-antibody complex (horse radish-peroxidase) and its use in the identification of spirocheyes. *J. Histochem. Cytochem.* 18:315–333.

62. Tapscott, S. J., G. S. Bennett, Y. Toyama, F. A. Kleinbart, and H. Holtzer. 1981. Intermediate filament proteins in the developing chick spinal cord. *Dev. Biol.* 86:40–54.

63. Tapscott, S. J., G. S. Bennett, Y. Toyama, F. A. Kleinbart, and H. Holtzer. 1981. Intermediate filament proteins in the developing chick spinal chord. *Dev. Biol.* 86:40–54.

64. Tokayasu, K. T., P. A. Maher, A. H. Dutton, and S. J. Singer. 1985. Intermediate filaments in developing myotubes in vitro. *J. Cell. Biochem. Suppl.* 9b:82a.

65. Tokayasu, K. T., P. A. Maher, and S. J. Singer. 1984. Distributions of desmin and vimentin in developing chick myotubes in vivo. I. Immunofluorescence study. *J. Cell Biol.* 98:1961–1972.

66. Tokuyasu, K. T., P. A. Maher, and S. J. Singer. 1985. Distributions of vimentin and desmin in developing chick myotubes in vivo. II. Immunoelectron microscopic study. *J. Cell Biol.* 100:1157–1166.

67. Toyama, Y., S. Forry-Schaudies, B. Hoffman, and H. Holtzer. 1982. Effects of taxol and colcemid on myofibrillogenesis. *Proc. Natl. Acad. Sci. USA.* 79:6556–6566.

68. Vertel, B., and D. A. Fischman. 1976. Myosin accumulation in mononucleated cells of chick muscle cultures. *Dev. Biol.* 48:438–446.

69. Wang, K., J. Ash, and S. Singer. 1975. Filamin, a new high-molecular weight protein found in smooth muscle and non-muscle cells. *Proc. Natl. Acad. Sci. USA.* 72:4483–4486.

70. White, G., M. Gimbrone, Jr., and K. Fujiwara. 1983. Factors influencing the expression of stress fibers in vascular endothelial cells in situ. *J. Cell Biol.* 97:416–424.

71. Wulf, E., A. Deboben, F. A. Bautz, H. Faulstich, and T. Wieland. 1979. Fluorescent phallotoxin, a tool for visualization of cellular actin. *Proc. Natl. Acad. Sci. USA.* 76:4498–4502.

72. Zigmond, S. H., J. J. Otto, and J. Bryan. 1979. Organization of myosin in a submembranous sheath in well-spread human fibroblasts. *Exp. Cell Res.* 119:205–219.